



DESIGN AND ANALYSIS OF SOLAR POWER GENERATOR SYSTEM WITH A NEW METHOD

**A THESIS SUBMITTED TO
THE GRADUATE SCHOOL OF APPLIED
SCIENCES
OF**

NEAR EAST UNIVERSITY

By

Hayder Hassan Abbas

**In Partial Fulfillment of the
Requirements for the Degree of Master of Science
in
Electrical and Electronic Engineering**

Nicosia - 2013



**Hayder Hassan Abbas : Design and Analysis of a Solar Power Generator
System with a New Method**

**Approval of Director of Graduate School of
Applied Sciences**


Prof. Dr. İlker SALİHOĞLU

**We certify this thesis is satisfactory for the award of the degree of Masters
of Science in Electrical and Electronic Engineering**

Examining Committee in Charge:


Prof. Dr. Sezai Dinçer

Electrical & Electronic
Engineering Department, NEU


Assoc. Prof. Dr. Özgür Cemal Özerdem

Electrical & Electronic
Engineering Department, NEU


Assist. Prof. Dr. Tayseer Alshanableh

Electrical & Electronic
Engineering Department, NEU


Assist. Prof. Dr. Lida Vafaei

Mechanical Engineering
Department, NEU


Dr. Samet Biricik

Electrical & Electronic
Engineering Department, EUL


Assoc. Prof. Dr. Özgür Cemal Özerdem,

Supervisor, Electrical &
Electronic Engineering
Department, NEU

DECLARATION

I hereby declare that all information in this document has been obtained and presented in accordance with academic rules and ethical conduct. I also declare that, as required by these rules and conduct, I have fully cited and referenced all material and results that are not original to this work.

Name: Hayder Hassan Abbas

Signature: 

Date: 10 June 2013

ABSTRACT

Global warming is currently a worldwide concern due to the rising pollution in the ecosystem; this is a result of the ever-increasing demand for electricity which depends on fossil fuel. Therefore, using other renewable energy resources such as solar energy has been investigated as an alternative power generating resource in the past few decades.

The main purpose of this thesis is to develop a solar panel model, which gives a real operation condition according to IEC standard and real life recorded data. Therefore, two models are implemented, developed, and validated. The DC / DC converter is implemented and studied under different operation conditions, an AC / DC inverter is presented and studied for solar energy application. In this thesis a novel approach was presented by the use of back of the panel temperature to measure and calculate the solar model parameters which mimic the real operation of a PV cell. Finally MATLAB simulator 2012a version is used to design and simulate a solar power generators for domestic load, the result of implemented circuit is discussed in details.

Keywords: Solar energy, solar panel model, DC/DC converter, AC/DC inverter, solar power for domestic load

*Dedicated to the memory of my mother, with love to my wife,
daughter (Fatima), and son (Diyar).*

ACKNOWLEDGMENTS

First of all, I want to thank God for giving me the fortitude to complete this study, secondly, I would like to express my sincere gratitude to my supervisor Assoc. Prof. Dr. Özgür Cemal ÖZERDEM for his helpful efforts, fruitful guidance, and continual encouragement throughout the entire work.

Thirdly, my thanks and appreciations go to Prof. Dr. Adnan KHASHMAN, who provided me with extensive input, alternative views and he put me on the correct path of becoming a researcher.

Special thanks to my wife for her kindness, support encouragement and patience,

Finally, it is an honor for me to have the opportunity to say a word to thank all people who helped me to complete this work, although it is impossible to include all of them here.

TABLE OF CONTENTES

DECLARATION.....	ii
ABSTRACT	iii
ACKNOWLEDGMENTS	v
TABLE OF CONTENTES	vi
LIST OF TABLES	viii
LIST OF FIGURES	ix
ABBREVIATIONS USED	xi
CHAPTER ONE: INTRODUCTION	1
1.1 Overview.....	1
1.2 Introduction	1
1.3 Literature review	3
1.4 Thesis Objectives	7
1.5 Thesis organization	8
CHAPTER TWO: SOLAR ENERGY	9
2.1 Overview	9
2.2 Diffuse and Direct Solar Radiation	9
2.3 Solar constant (Irradiance)	11
2.4 Solar Energy Power Generation	12
2.4.1 Solar Thermal Electricity Generation	12
2.4.2 Photovoltaic PV (Solar cell)	13
2.5 Photovoltaic Module connections	15
2.6 Photovoltaic (PV) generations	16
2.7 Types of Photovoltaic Cells	16
2.8 Photovoltaic Applications	17
2.9 Photovoltaic Topologies	19
2.10 Characteristics of a PV Cell	21
2.11 PV Cell Model	22
2.12 PV Cell Model Implementation	24
2.12.1 Model One	24
2.12.2 Model Two	27
2.13 Photovoltaic Array Modeling	31
CHAPTER THREE: POWER ELECTRONIC DEVICES	33
3.1 Overview	33
3.2 Power Electronics	33
3.3 Power Electronics Converters	34
3.4 DC/DC Converter	36
3.5 DC/DC Converter Types	36
3.5.1 Buck Converters	36
3.5.2 Boost Converters	38
3.5.3 Buck-Boost Converters	39
3.5.4 Cuk converter.....	40

3.6 Maximum power point Tracking controller and algorithm	40
3.6.1 Different MPPT techniques	41
3.6.2 Perturb and observe	42
3.7 Inverter	44
3.7.1 Classification of Voltage Source Inverters	44
3.7.2 Inverter Configuration	44
3.7.3 Solar Inverters	46
3.7.4 Inverter Topology in PV System	46
3.8 Proposed Simulation	49
3.8.1 PHASE TWO: MPPT and DC/DC Converter	49
3.8.2 PHASE THREE: DC/AC Inverter	57
CHAPTER FOUR: Experimental and Simulation Results	60
4.1 Overview	60
4.2 Experimental Work	60
4.3 Simulation Work	62
4.3.1 Phase One: PV array models	63
4.3.2 Phase Two: DC/DC converter with MPPT	70
4.3.3 Phase Three: DC/AC inverter	74
4.4 Solar Power Generator Design for Domestic Load	75
4.5 Results Discussion	82
4.5.1 Phase One: PV modeling	82
4.5.2 Phase Two: DC/DC converter with MPPT controller	82
4.5.3 Phase Three: DC/AC inverter	82
CHAPTER FIVE: CONCLUSIONS and FUTURE WORK	84
CONCLUSIONS	84
FUTURE WORK	85
REFERENCES	86
APPENDICES	92

LIST OF TABLES

4.1	The data sheet manufacture of NT 111 solar panel	62
4.2	Shows the unknown parameters by first model	66
4.3	Shows the unknown parameters by second model	68
4.4	The experimental, model one, and model two results	70
4.5	The calculated parameters values of DC/DC converter	71
4.6	L-C Experimental values of DC/DC converter	71
4.7	Shows the test data for implemented MPPT system	76
4.8	The day length and clearness index	78
4.9	Average seasons solar irradiance in study area	78
4.10	Shows the variables used to configure the DC/DC converter	79

LIST OF FIGURES

2.1	Diffuse and direct Solar Radiation Source.....	10
2.2	Earth's atmospheric effect on the solar radiation attenuation	12
2.3	Solar thermal plant Source	13
2.4	Components of PV Cell Source	14
2.5	Photovoltaic Cell, Module, and Array Source	14
2.6	Modules in series	15
2.7	Modules in parallel	15
2.8	Example silicon cell in panel.....	17
2.9	Example of PV's application.....	19
2.10	The standard topology of PV system	20
2.11	I-V and PV curve characteristics	22
2.12	PV module equivalent circuit	23
2.13	The circuit diagram of PV model	26
2.14	Implemented circuit diagram of PV model.....	27
2.15	Implemented circuit diagram of PV model.....	27
2.16	Flow chart of second modeling circuit.....	30
2.17	PV array composed of $N_s * N_p$ cells (module).....	31
3.1	Power ratings and switching speeds of the controlled semiconductor	35
3.2	Semiconductors power electronic devices	35
3.3	Buck converter circuit diagram	37
3.4	Output voltage and current waveforms	37
3.5	Boost converter circuit diagram	38
3.6	Waveforms of source current	38
3.7	Buck-boost converter circuit diagram	39
3.8	Inductor current (I_L) waveform	39
3.9	Cuk converter circuit diagram	40
3.10	The P-V curve showing MPP and operating points	42
3.11	Flow chart of the P&O algorithm	43
3.12	Inverter configuration	45
3.13	PV plant different connecting topology	48
3.14	AC module configuration of a photovoltaic generator	48
3.15	The proposed design phases	49
3.16	The schematic diagram of the photovoltaic simulation system	50
3.17	Block Diagram of MPPT control box	50
3.18	Schematic diagram of Buck-Boost converter	51
3.19	The two operating states of a buck-boost converter	52
3.20	Waveforms of I and V in a buck-boost converter (continuous mode)	54
3.21	Waveforms of I and V in a buck-boost converter (discontinuous mode)	57
3.22	Topology of a single-phase inverter with filter and load	58

3.23	Output current for S1, S2 ON; S3, S4 OFF for $t_1 < t < t_2$	58
3.24	Output current for S3, S4 ON; S1, S2 OFF for $t_2 < t < t_3$	59
4.1	PV panels	61
4.2	Variable resistance (BOX 1051)	61
4.3	Explorer GLX	61
4.4	Implemented circuit diagram of PV model	62
4.5	Implemented circuit diagram of PV model	63
4.6	The internal circuit diagram of PV array model one	64
4.7	The complete circuit diagram of a PV array	64
4.8	The I-V curve of implemented circuit model one	65
4.9	The P-V curve of implemented circuit model one	65
4.10	The circuit diagram of model two	67
4.11	The internal circuit diagram of PV array model two	67
4.12	The block diagram of PV array model two	68
4.13	Comparison between modeling results and experimental	69
4.14	The schematic diagram of the photovoltaic simulation system	70
4.15	The circuit diagram of buck boost converter	71
4.16	Simulation Result of case 1	72
4.17	Simulation Result of case 2	73
4.18	Simulation Result of case 3	73
4.19	Simulation Result of case 4	74
4.20	Implemented circuit of DC/AC converter	74
4.21	Simulation results waveforms of the load voltage and current	75
4.22	Parallel connection of PV	79
4.23	Series connection of PV	79
4.24	Internal components of PV panel	80
4.25	Inverter connected with PV panel	81
4.26	Simulation waveform of implemented system for domestic load	81

ABBREVIATIONS USED

a	Diode Ideality Constant.
AC	Alternating Current.
AU	Astronomical Unit.
BJT	Bipolar Junction Transistor
DC	Direct Current.
E	Solar Irradence.
E_{beam}	Directional Solar Irradiance.
E_{dir}	Direct Solar Irradiance.
FET	Field Effect Transistor.
GTO	Gate Turn Off.
IGBT	Insulated Gate Bipolar Transistor.
I_m	Current at maximum power.
InC	Incremental Conductance.
I_o	Leakage Current of The Diode.
I_{ph}	Photovoltaic current.
I_{sat}	Saturation Current of The Diode.
I_{sc}	Short circuit current at nominal tempearture.
$I_{\text{sc,nom}}$	Short circuit current.
K_p	short circuit current factor.
K_v	open Circuit Voltage factor.
MOS	Metal Oxide Semiconductor.
MOSFT	Metal Oxide Semiconductor Field Effect Transistor.
MPPT	Maximum Power Point Tracking.
N_p	Number of parallel cells.
N_s	Number of series cells.
P&O	Perturb & Observe.
PV	Photovoltaic.
PWM	Pulse Width Modulation.
R_p	Parallel Resistance of PV Panels.
R_s	Series Resistance of PV Panels.
SCR	Silicon Controlled Rectifier.

Si	Silicon.
STC	Standard Test Conditions.
TF	Tracking factor.
T_T	Temperature at (25°C).
V_m	Voltage at maximum power.
V_{oc}	Open Circuit Voltage.
V_{ph}	Photovoltaic Voltage.
V_t	Thermal voltage of diode.
Φ	Angle of Incidence.

CHAPTER ONE

INTRODUCTION

1.1 Overview

This chapter is composed of an introduction to the thesis where a literature review is done and the objectives and the outline are discussed in details besides a block diagram of the thesis plan is given.

1.2 Introduction

As a matter of fact no one can deny that electricity is an important part in our everyday life. Furthermore, electricity actually plays an essential role in the development of industry, agriculture, medicine and all fields of human activities. The global primary electric energy demands are met largely from conventional energy source as fossil fuels, which add to environmental degradation problems through gaseous emissions, using renewable and unconventional energy power sources will help to control, replace and avoid adverse environmental impacts [1, 2, 3].

The Solar energy is an inexhaustible resource, where the sun produces vast amounts of renewable solar energy that can be collected and converted into heat and electricity. The ecological life depends on the sun's energy. Which is very important for the chemical and biological processes on our planet [4, 5]. "It is an established and accepted fact that solar energy will play an increasingly important role in the future as it is cleaner and easier to use and environmentally being and is bound to become economically more viable with increased use"[6].

The importance of solar energy is outlined by [7] in the following points: Renewable and free, Safe and clean. Less maintenance required, Cost-effective in remote areas, Provides energy independent of the power grid, and Flexible and adaptable.

From the 50's of the last century scientists are trying to find a new technology to generate clean energy. The sun is considered to be the most important one because it's clean and renewable source through use of Photovoltaic cells which were convert sunlight to electricity. A photovoltaic (PV) is the most promising one as a future energy technology [8, 9, 10] and has less operational and maintenance costs [11, 12].

In general, the basic elementary device used in PV systems is the PV cell; a PV cell is consisting of semiconductor material which directly converts sunlight into electricity [13]. A group of cells interconnected in series or parallel to form a new building block so called PV module [14]. The modules are then connected together depending upon required voltage and current and general series and parallel topologies are used in order to increase voltage and current respectively. A PV array is formed by series and parallel combinations of modules and the produced power is direct current (DC) [15].

However, in photovoltaic power generator system the interface between source (solar array) and load (utility grid) consists of three stages, which are solar array, the DC-DC converter with a maximum power point tracker (MPPT), and inverter. In order to study the characteristic of a PV system modeling of the PV array is necessary.

A PV device is a nonlinear device and the characteristic of generating power depend essentially on solar irradiance and cell temperature [2, 11, 15]. The system can be mathematically modeled based on the theoretical equations that describe the functioning of the PV system using the equivalent circuit [9, 16, 11]. The equivalent circuit of a single solar cell could be modulated by using one current source, one diode or two diodes when more accuracy is required, and parallel resistor (R_p) with series resistor (R_s) connected in series [16].

Due to the nonlinear characteristics of PV cell with weather and load condition on one side and the high capital cost of PV array on other, maximum power point tracking (MPPT) control technique is essential in order to extract the maximum available power from PV

array in order to maximize the efficiency of PV array [12, 17]. Therefore, the MPPT is used to control a DC/DC converter which inserted between PV generator and inverter circuit. The role of MPPT algorithms controls the switching of DC-DC converter by applying pulse-width modulation (PWM) technique [17, 18].

The last part of a standalone PV power system is an AC / DC inverter; the main function of the inverter changes the generated voltage from the PV from DC to AC to be used in supplying normal AC load for household and industrial appliances which need AC current.

In this thesis several PV modules are proposed and simulated, the best model is selected according to the empirical result and validation data. To validate the selected model, these data that consist of voltage, current, temperature, and solar irradiance were recorded.

Thereafter, the selected module of PV array will be connected with DC/DC converter controlled by MPPT algorithm, and the better MPPT algorithm and DC/DC converter will be selected according to literature survey.

Finally the DC/AC inverter will be designed to achieve AC current in the final stage of PV system, where the best design will be selected according to the simulation result. After that, a small scale PV power system implemented and validated to supply the domestic load.

1.3 Literature review

This section includes research papers and published articles related to modeling of PV systems. Many parameters affected the operation of PV, to calculate some parameters which uncovered by data sheet has been addressed by few research works. For instance, in [2], the authors implemented a generalized photovoltaic model using Matlab/Simulink, which is representative of a PV cell, module, and array; the proposed model connected to power electronics for a maximum power point tracker. Taking the effect of sunlight irradiance and cell temperature into consideration, they assumed that $R_s = 0$ and $R_p = \infty$ for easy calculation and to approximate the results.

Using an incremental conductance method for MPPT algorithm theory presented in [4] where Matlab Simulink used, to simulate a Solar Photovoltaic module using The I-V and PV characteristics are obtained for various values of solar insolation keeping the cell temperature constant. They proposed for further work using the proposed simulation model in conjunction with MPPT algorithm can be used with DC-DC Boost converter. The authors in [11] study the use of numerical methods to find such parameters which are not provided by the manufacturers data sheet, for example R_s , R_p , A , I_o , I_{sat} , by using internal parameters were given in the PV module datasheet, they present a new improvement and modification for some of the existing models under standard test condition (STC) and under varying environmental conditions.

In [15] a solar cell single diode model parameters from experimental data were extracted, the author suggested a number of methods for measuring the series resistance (R_s) of a solar cell, other parameters, such as R_p , I_{sat} , and ideality factor of a diode (a) at a particular temperature and solar irradiance can be computed from the other parameters which were provided by the manufacturer data sheet of PV panel.

The Authors in [18] have proposed a method for modeling a photovoltaic array, they calculate unknown parameters of PV array by adjusting the nonlinear $I-V$ curve at three points: maximum power (V_m), short circuit (I_{sc}), and open circuit (V_{oc}). These three points provided by the manufacture PV array datasets, the method finds the best $I-V$ equation for the single-diode photovoltaic model including the effect of the series and parallel resistances, and warranties that the maximum power of the model matches with the maximum power of the real array, they present a simple, fast, accurate, and easy-to-use modeling method for using in simulations of PV systems.

In order to validate the MATLAB simulated model of PV array presented in [19], the proposed model is based on mathematical equations, to find out the equivalent circuit of PV array which includes a photocurrent source, a diode, a series resistance (R_s) and a parallel resistance (R_p). The developed model allows the prediction of PV cell behavior under different physical and environmental parameters. They presented that the obtained results are in good agreement with the simulation ones. The authors in [20] proposed a model of a PV array, which uses only parameters given by manufacturer datasheets

without the use of any numerical calculation, they suggested that the electrical parameters of the modules can be changed and it will be different from those given by the manufacturer when the PV Array is getting older. Therefore, the behavior of the mathematical model of a PV module can't match the real operating conditions. The simulated model based on Shockley diode equation to build an accurate PV module.

An electric model is presented in [21] the electrical model consists of photo-current current source, a single diode junction and a series resistance, and also includes temperature dependences, this model is used to investigate the variation of maximum power point with temperature and insulation levels. A comparison of buck versus boost MPPT topologies is made, and compared with a direct connection to a constant voltage (battery) load. The boost converter shows it has a slight advantage over the buck, since it can always track the maximum power point.

A simple inverter consists of one stage single phase was presented in [22] the inverter connected with DC-DC converter which integrated the MPPT, also the authors have presented, the control approach which based on the current and voltage amplification. They show that using two DC/DC converters connected to a common inverter, which has more advantages than using centralized DC/DC converter, the designed topology considers a suitable for small or large-scale solar power generator.

In [23] a complete solar power generator system was presented which consists of PV panel, an MPPT controller with DC/DC buck converter, and inverter, and cloud generation. They developed two systems in this study: first, a centralized MPPT for all PV's and the second strings MPPT connected with each panel in the array individually. For each system, a best case and worst-case weather scenario were run. The performance of each system was observed and compared. The authors investigated that the performance of distributed MPPT is better than the centralized one in the cloudy weather situation but in the sunny day there is no difference between the two systems.

Two MPPT algorithms developed in [24] used to control a high efficiency of DC-DC converter, the MPPT algorithms were used are Incremental Conductance (INC) method and Perturbation and Observation (P&O) method are applied to the converter. The

simulation results of 3kW PV array together with the converter show that the P&O method is more appropriate than the INC method because it gives a higher speed and accuracy of system performance.

In [25] the authors have presented a low-cost implementations of the P&O maximum power point tracking algorithm, they developed a new method to limit the negative effects of P&O algorithm which are, at steady state, the operating point oscillates around the MPP giving rise to the waste of some amount of available energy, also the P&O algorithm can be confused during those time intervals characterized by rapidly changing atmospheric conditions, they suggested that the P&O MPPT parameters must be customized to the dynamic behavior of the specific converter adopted in order to avoid the negative effects of P&O algorithm.

In [26] the authors implemented several MPPT algorithms to evaluate the best performance among the most commonly used of MPPT techniques, making meaningful comparisons with respect to the amount of energy extracted from the photovoltaic panel tracking factor (TF) in relation to the available power. The experimental results are presented for conventional MPPT algorithms and improved MPPT algorithms named IC based on proportional–integral (PI) and perturb and observe based on PI, finally the table of comparison showed that the P&O algorithm has a simple circuit implementation, good accuracy, and good tracking factor.

In [27] the authors developed a photovoltaic simulation system with MPPT function using Matlab/Simulink software in order to simulate and evaluate the behaviors of the real photovoltaic systems. After that, a DC/DC buck-boost converter with two different MPPT algorithms established and simulated. The research found that P&O algorithm possesses faster dynamic response than INC algorithm owing to its simple judgment procedure in every perturbing period.

All these recent works aimed of modeling a PV System by using MATLAB simulated package, and mathematical equations were used for modeling a single solar cell, in [2], [20] the authors neglecting the parallel resistor and series resistor of solar cell, but in [4], [11, 18, 19, 23, 24] the authors take in their consideration R_s and R_p and they highlighted

the effect of these resistors on the output of PV array specially when there is validation data (real time recorded data) which compared with simulated result. Also the authors in [24, 25, 26, 27] are presented that the two very common MPPT algorithms are INC and P&O, these two algorithms are shared same features which are , simple circuit implementation, low cost implementations, higher speed and accuracy of system performance.

In [27] the authors used P&O with INC algorithm to control the DC/DC converter they found that the best structure was a Buck - boost converter. In [22] the authors found that the using individual DC/DC converter with each PV panel is better than used centralized DC/DC converter for PV's. Also in the same article [22] the authors proposed a single-phase inverter, which are, consist from full bridge circuit, they proved that the proposed inverter is suitable for large-scale solar power generator.

Therefore, in this thesis MATLAB simulated package will be used to simulate the PV array, and P&O algorithm will be used to control a DC/DC converter to achieve MPPT , also a single phase inverter is presented by using the PI controller for the PV modeling system.

The final judgment about the best PV model, MPPT algorithm, will be according to the simulation result and validation data to validate best circuit design.

1.4 Thesis Objectives

The main objectives of this thesis are

1. To study the different circuits of PV array in order to select the best one.
2. To design and study a DC/DC converter, and MPPT algorithms for PV application.
3. To study a DC/AC inverter for PV application.

The ultimate objective of this thesis is to build a solar power generator in small scale to supply a householder in the Koya city (KRG of IRAQ); this will be developed by using MATLAB Simulink environment based on real life data recorded.

1.5 Thesis organization

The thesis has been organized into five chapters.

Chapter One: is an introduction of the thesis. This chapter provides the introduction of the thesis, literature reviews, thesis objectives, thesis organization, finally a block diagram that describes the organization of the thesis.

Chapter Two: Focuses on solar energy, application, PV (cells, panel, and array), types of solar cells, and the modeling equations, which are used to build a simple solar cell , where two models of solar cell module are given.

Chapter Three: Explains power electronic devices, MPPT concept and algorithms, an introduction to DC/DC converter with focusing on buck-boost converter, and finally DC/AC inverter with controlling strategies are given.

Chapter Four: Experimental and implementation result discussed and compared with simulation results of the overall PV power generator.

Chapter Five: Draws a conclusion for this dissertation and proposes future work. The recommendation is also discussed in this Chapter.

CHAPTER TWO

SOLAR ENERGY

2.1 Overview

In this chapter, the following topics will be discussed: diffuse and direct solar radiation, solar constant, and solar applications, thermal and electric forms. In addition to PV cell types, application, PV array model, topology, and proposed modeling.

2.2 Diffuse and Direct Solar Radiation

The most important supplier of energy for Earth is the sun. The whole life depends on the sun's energy. It is the starting point for the chemical and biological processes on our planet. At the same time it is the most environmentally friendly form of all energies, it can be used in many ways, and it is suitable for all social systems [28]. The Sun is made up of about (80) % hydrogen, (20) % helium and only (0.1) % other elements. Its Radiant power comes from nuclear fusion processes, during which the Sun loses 4.3 million tons of mass each second, to be converted into radiant energy [29]. As sunlight passes through the atmosphere, some of it is absorbed, scattered, and reflected by the following: [29]

- Air molecules
- Water vapor
- Clouds
- Dust
- Pollutants
- Volcanoes

This is called diffuse solar radiation. The solar radiation that reaches the Earth's surface without being diffused is called a direct beam solar radiation. The sum of the diffuse and direct solar radiation is called global solar radiation. Atmospheric conditions can reduce

direct beam radiation by (10)% on clear, and dry days and by (100)% during thick, and cloudy days [29].

In other words, on a clear day the amounts of diffuse energy are (15-20) % of global irradiance whereas on a cloudy day it will be (100) %, sunlight that reaches the earth's surface without scattering is called direct or beam radiation. Scattered sunlight is called Albedo radiation, and the sum of all three components of sunlight is called global radiation [27].

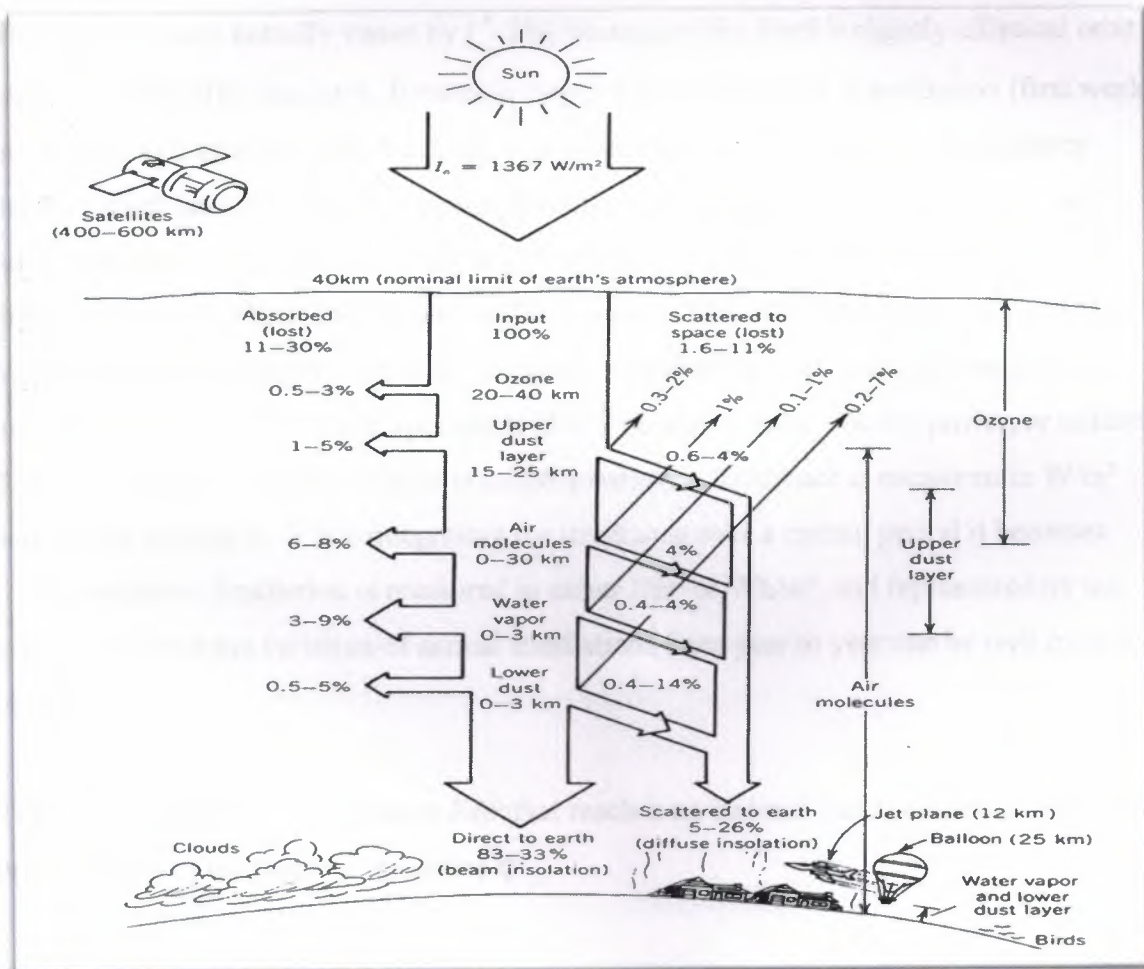


Figure 2.1 Diffuse and direct Solar Radiation Source [30].

2.3 Solar constant (Irradiance)

The solar constant is defined as the quantity of solar energy (W/m^2) at normal incidence outside the atmosphere (extraterrestrial) at the mean sun-earth distance. Applying the Stefan-Boltzmann's law to the Sun and Earth the radiant flux, received from the Sun outside the Earth's atmosphere can be calculated as a mean value of (1367.7 W/m^2) [31]. Solar constant acquires special importance in the applications of solar energy so that it cannot in fact access to the amount of energy from the sun is higher than the value of solar constant [32].

The solar constant actually varies by ($\pm 3\%$) because of the Earth's slightly elliptical orbit around the Sun. The sun-earth distance is larger when the Earth is at perihelion (first week in January) and smaller when the Earth is at aphelion (first week in July), the distance between earth and sun is another factor affecting solar radiation, and the variation, and refers to the solar constant as the power per unit area received at the average Earth-solar distance of one "Astronomical Unit" or AU which is (149.59787066) million kilometers. Various different measurement units are used when dealing with solar radiation, often incorrectly even by some solar specialists [33]. The total specific radiant power, or radiant flux, per area that reaches a surface is called Irradiance. Irradiance is measured in W/m^2 and has the symbol E . When integrating the irradiance over a certain period it becomes solar irradiation. Irradiation is measured in either J/m^2 or Wh/m^2 , and represented by the symbol H . Since the variation of annual irradiances from year to year can be well over 20 % [32].

The specific direct solar irradiance E_{dir} that reaches an inclined surface is lower depending on the cosine of the angle of incidence ϕ :

$$E_{\text{dir}} = E_{\text{beam}} \cos \phi \quad (2.1)$$

This is illustrated in Fig. 2.2 where it can be seen that for with increase of the angle ϕ the same radiation power covers a larger area, thus decreasing the irradiance as per area value.

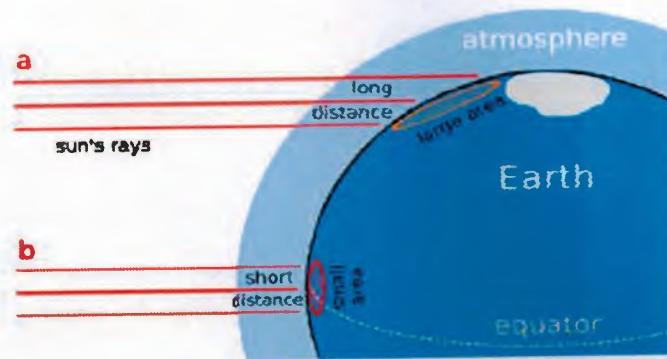


Figure 2.2 Earth's atmospheric effect on the solar radiation attenuation [32].

2.4 Solar Energy Power Generation

At the present time, solar energy can be harnessed in many ways, including using it for water heating, solar heating and cooling of buildings, crop and vegetable drying, and greenhouse agriculture. The solar radiation can be captured and converted into useful forms of energy, such as heat and electricity [34], this thesis focus on using solar energy to generate electricity. There are two ways to generate electricity from the sun which are:

2.4.1 Solar Thermal Electricity Generation

Solar thermal energy can be collected at large scale and complex collectors are generally used in solar power plants where solar heat is used to generate electricity by heating water to produce steam which drives a turbine connected to an electrical generator. Light from the sun may be collected using huge mirror arrays focused onto a receiver at the top of a tower [34].

Most commercially attractive is the solar thermal electricity generation system developed by Luz, which uses parabolic reflectors to warm heat-transfer oil running through a pipe at the focus of the reflector. This heated oil is used to raise steam to power a turbine [34].

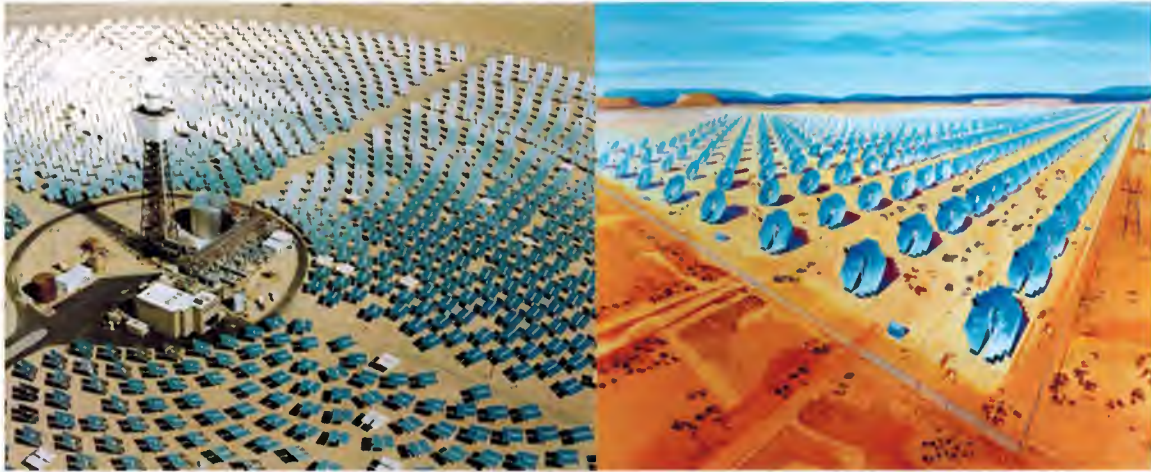


Figure 2.3 Solar thermal plant Source [30].

2.4.2 Photovoltaic PV (Solar cell)

Photovoltaic (PV) or Solar cell is a Semiconductor material that converts sunlight to electricity. Common seals are Silicon. The photovoltaic process does not produce any emissions; PV's have played an important role in our life, such as feeding satellites with needed electricity and they have many applications. The simplest solar cells provide small amounts of power for watches and calculators. More complex systems can provide electricity to houses and electric grids. Usually though, solar cells provide low power to remote, unattended devices such as buoys, weather and communication satellites, and equipment aboard spacecraft [35, 36].

2.4.2.1 How to produce electricity by photovoltaic cell?

Photovoltaic cell made from at least two layers of the semiconductor material which is usually silicon. A positive layer which is called p-type, the other layer negative which is called n-type, and between them an area that is called p-n junction [36, 37].

When light enters the cell, some of the photons from the light are absorbed by the semiconductor atoms, freeing electrons from the cell's negative layer (n-type) to flow through an external circuit and back into the positive layer (p-type) this flow of electrons

produces current [38, 39]. Typically , a PV cell generates a voltage around (0.5) to (0.8) volts depending on the semiconductor and the built-up technology [10, 40], these cells are connected with each other in a sealed so-called module. When two modules are connected with each other in series the voltage will be doubled, while the current remains constant, but when two modules are connected in parallel the current will be doubled and the voltage remains constant [40].

For the current and the voltage that be required many numbers of modules are connected to each other in a series and parallel form which is called an array. The following figures shows photovoltaic cell, module, and array [40].

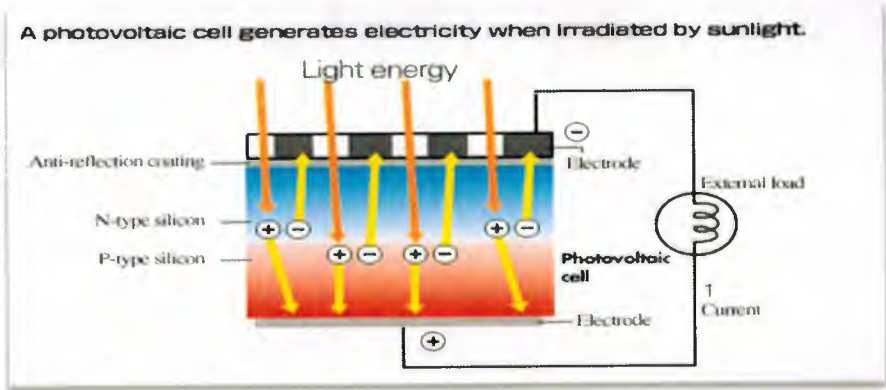


Figure 2.4 Components of PV Cell Source [30].

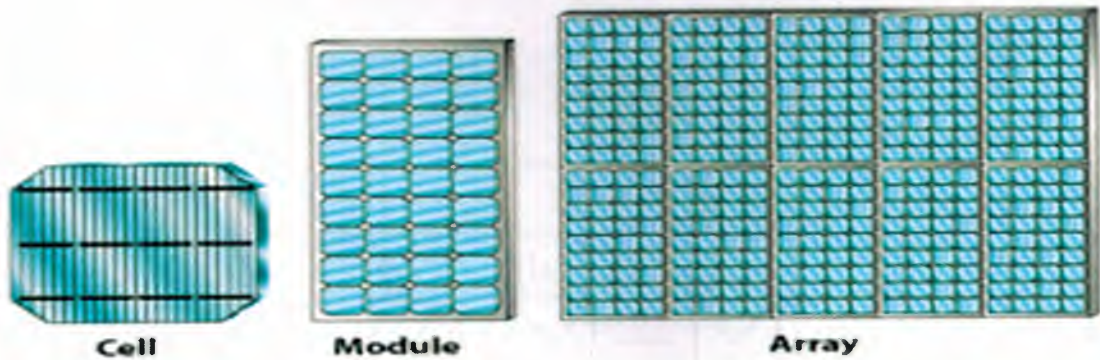


Figure 2.5 Photovoltaic Cell, Module, and Array Source [30].

2.5 Photovoltaic Module connections

Modules in series: When photovoltaic modules are connected in series increasing the voltage of the system. The final system voltage is the sum of the individual voltages of each module [41].

$$V_{\text{total}} = V_1 + V_2 + V_3 + \dots + V_n \quad (2.2)$$

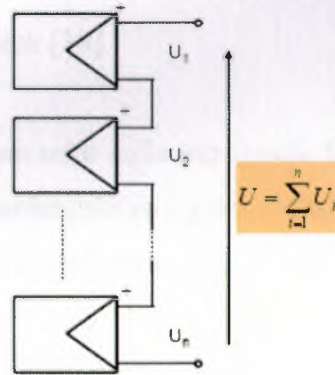


Figure 2.6 Modules in series [41].

Modules in parallel: Photovoltaic modules are connected in parallel to increase the current of the system. The final current is the sum of the individual currents of each module [41].

$$I_{\text{total}} = I_1 + I_2 + I_3 + \dots + I_n \quad (2.3)$$

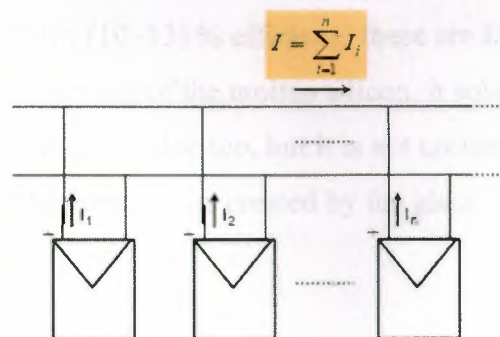


Figure 2.7 Modules in parallel [41].

2.6 Photovoltaic (PV) generations

The first generation of PV cells was discovered at Bell Telephone in 1954, when scientists discovered that silicon (is one of element found in sand) created an electric charge when exposed to sunlight [39]. Traditional solar cells are made from silicon, one of the most common elements on Earth [35]. Second-generation of PV cells changed names of PV cells into thin film solar cells because they are made from amorphous silicon or non-silicon materials such as Cadmium Telluride Thin film solar cells use layers of semiconductor materials only a few micrometers thick [39].

The last generation is third-generation solar cells were made from a variety of new materials besides silicon, including solar inks using conventional printing press technologies, solar dyes, and conductive plastics [42].

2.7 Types of Photovoltaic Cells:

There are four types of photovoltaic cells categorized according to silicon crystal and efficient rate and cost of production : [35, 39, 40, 43].

1. Monocrystalline silicon(15) % efficient, made up of sections of a single silicon crystal. When cooling, the molten silicon solidifies into a single large crystal, typically expensive to make (grown as big crystal).
2. Multicrystalline silicon (10–12) % efficient, these are formed by crystallized small particles. During the cooling of the molten silicon, it solidifies creating many crystals. Their appearance is blue too, but it is not uniform, since we can distinguish several different colors created by the glass , cheaper to make (cast in ingots).
3. Thin film silicon (4–6) % efficient, cheapest per Watt, easily deposited on a wide range of surface type.

4. Amorphous: These cells are produced when the silicon has not yet crystallized during processing, and it produces a gas that is projected onto a glass slide. They are able to operate with low diffuse light, even on cloudy days. The cost is much smaller and it can accommodate both flexible and rigid media. Against this, the performance, in full sunlight conditions, is between (5 -7) %, and it decreases, with the pass of time, around (7) %.

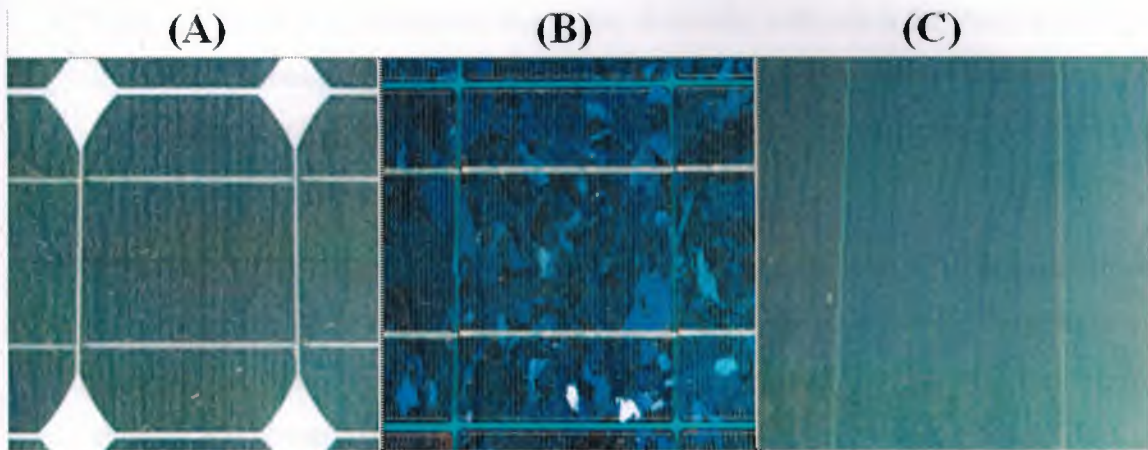


Figure 2.8 Example silicon cell in a panel, (A) single crystal silicon , (B) multicrystal Si., (3) amorphous Si [44].

2.8 Photovoltaic Applications

Photovoltaic system generates clean electric power, PV provides a suitable energy source for remote regions with no other electricity source. For example, photovoltaic systems can be used to supply electricity for: [45, 46, 47]:

1. Small scale such as domestic load or a large scale such as grid connected solar power plant.
2. Telecommunication repeater stations using of PV panel to power mobility, radio communication, telephones, remote control systems, emergency call boxes, microwave links, The range of power that is used in these systems varies from a few watts for an emergency call system to several kilowatts for large radio repeaters.

3. Aerospace application used PV panels to supply satellites, space station and telescopes which used in monitoring the space.
4. Water pumps: water pumping for irrigation, drinking, and small industrial purposes, this technique especially used in rural areas because, although the electricity is used as it is generated, the water can be stored in tanks during daylight hours and then using water by gravity when it was needed at night.
5. Village and remote residences: due to the electricity network is far away and the distance between the houses is large although, the number of population is few. The PV system supplies energy effectively for the operation of refrigerators, televisions, lightings, radios, etc.
6. Lighting: PV lighting is very common in remote locations such as nature preserves, mountain areas, highway signs, or rural towns and villages, street lighting, security, gardens, vacation cabins, and the car's sparking, these kinds of lighting systems are reliable and cheap cost.
7. Handle electronics devices: One of the uses of PV technologies is handling electronics that require low energy, such as watches, calculators, cameras, which are working well, even in normal light environments such as classrooms and offices.
8. Battery Charging: Photovoltaic system provides constant and small current to the batteries to prevent discharge problems. These PV cells are very reliable and a cheap solution in these cases.
9. Warning signal: PV is used to power warning signal in several areas such as the transportation, oil industries, utility and military. This warning signal that could be, highway warning signs, transmission tower, navigational beacons.
10. Remote observation: the applications of photovoltaic have become very large and observation system is one of these largest applications. PV systems are used to monitor the water, weather, temperature, flow rate and oil pipes.



Figure 2.9 Example of PV's application [30].

2.9 Photovoltaic Topologies

Photovoltaic systems can be grouped into stand-alone systems and grid connected systems. In stand-alone systems, the solar energy supplies the energy demand. Since the solar energy yield often does not match in time with the energy demand from the connected loads, additional storage systems (batteries) are generally used. If the PV system connected by another power source such as, a wind generator or diesel generator, this is known as a photovoltaic hybrid system. In grid-connected systems, the public electricity grid functions as an energy store [47] the overall topology shown in Fig. 2.10.

- Direct coupled PV system

In direct-coupled system, the PV array is connected directly to the load. Therefore, the PV operates only whenever there is solar radiation, so, this system has very limited application such as water pumping.

- Stand alone system (Off Grid)

Stand-alone system is used in areas have not access to a public grid , such as remote area and rural places, the produced energy usually stored in batteries. This system composed

from the PV array, batteries, charge controller, and sometimes inverter when AC current required.

- Grid connected system (On Grid)

Nowadays, the grid connected system is a usual practice to connect PV system with public grid, this means that “sunshine” system supplies the domestic, commercial, and industrial load, the remain of the harvested energy will be sold to one of electricity supply companies, this system usually composed from PV array and inverter.

- Hybrid connected system

In the hybrid system, more than one electricity generators are used with the PV system such as wind turbine and diesel generators, this system composed from the PV array, and inverter.

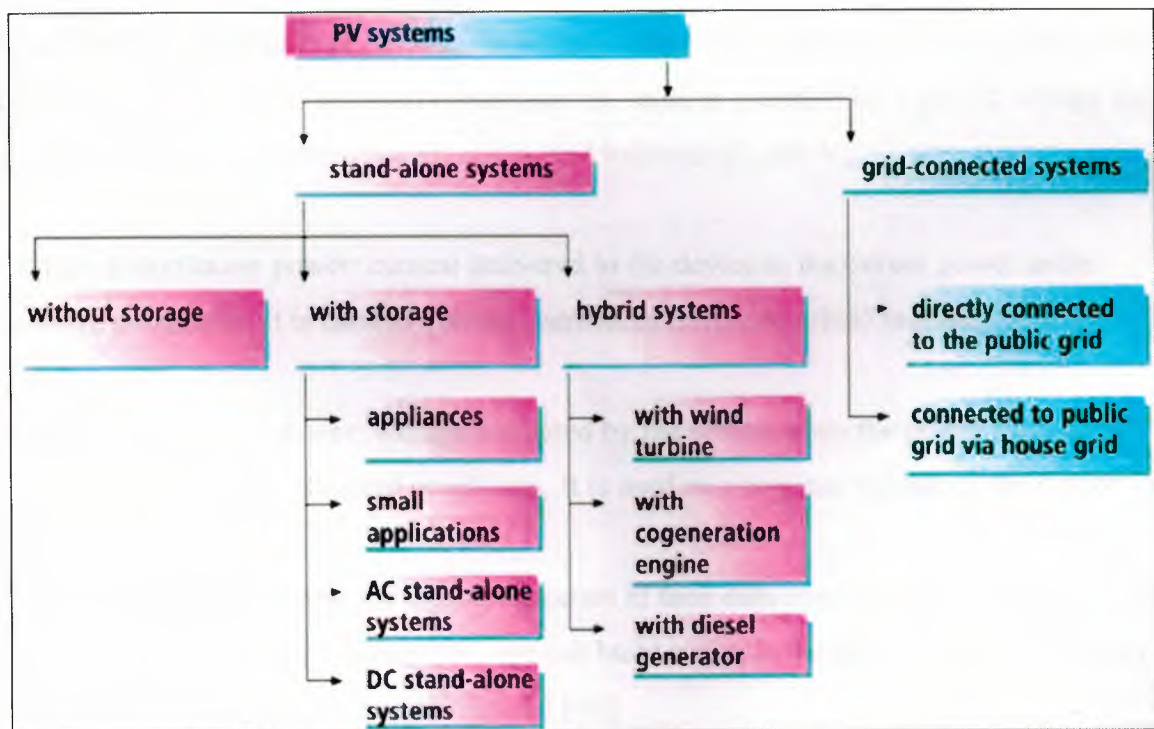


Figure 2.10 The standard topology of PV system [47].

2.10 Characteristics of a PV Cell

There are three parameters playing an important role in the study the characteristic of PV system, these are open circuit voltage (V_{oc}), short circuit current (I_{sc}) and maximum power point (P_{max}). The maximum power that can be supplied from a PV cell are at the maximum power points. These parameters are provided by the manufacture at standard test condition (STC) where the temperature (T) equal to (25°C), and solar irradiance equal to 1000 W/m^2 all parameters are described below [45]:

Short circuit current (I_{sc}): Maximum amount of current that can deliver the PV module under standard conditions, corresponding to zero voltage and therefore no power.

Open circuit voltage (V_{oc}): The maximum voltage that is delivered in a PV module under standard conditions, not allowing any current flow between the terminals of photovoltaic module under conditions of zero current and therefore no power.

Maximum or peak power (P_{max}): P_{max} is the maximum value of power that can be delivered by the PV module under standard conditions. Its value is specified by a pair of voltage and current values, ranging between (0) and I_{sc} and between (0) and V_{oc} .

Current at maximum power: current delivered to the device in maximum power under standard conditions. It is used as nominal current of the photovoltaic module.

Voltage at maximum power: voltage delivered by the device when the power reaches its maximum value under standard conditions. It is used as a nominal voltage of the device [48].

Usually manufacturers provide these parameters in their data sheets for a particular PV cell or module. By using these parameters, we can build a simple model but more information is required for designing an accurate model [48].

The current to voltage characteristic of a solar array is non-linear, which makes it difficult to determine the MPPT. The Fig. 2.11 gives the characteristic I-V and P-V curve for a fixed level of solar irradiation and temperature [49].

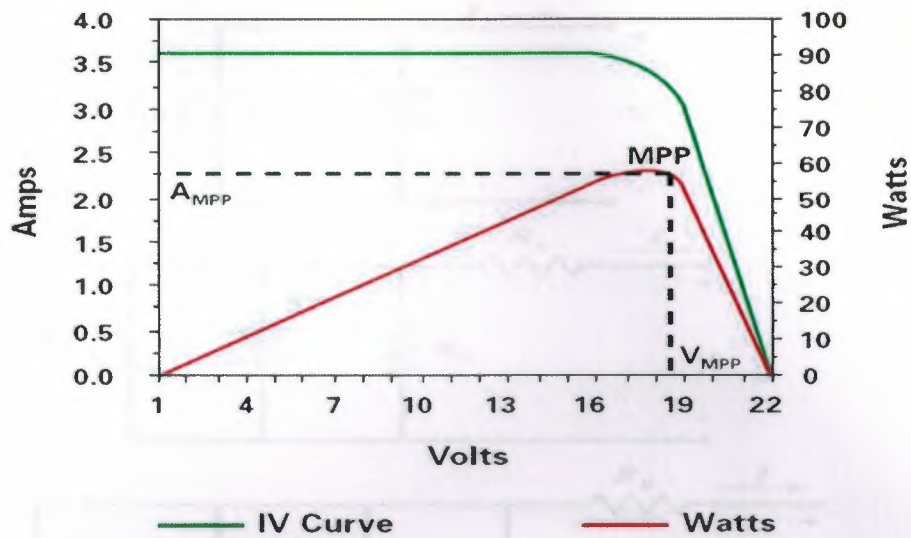


Figure 2.11 I-V and PV curve characteristics [49].

2.11 PV Cell Model

The equivalent circuit of a PV cell, models have been developed by many researchers in order to find accurate, simple, and practical model for PV module, in this regard the model can be mathematically modeled based on the theoretical equations that describe the functioning of the PV system using the equivalent circuit in the literature of this thesis.

Other models are empirically-based models that acquire their versatility and accuracy from the fact that individual equations used in the model are derived from individual PV system characteristics [11]. Fig. 2.11 (a) to (c) shows the equivalent circuit model used by researchers to describe the behavior of the PV module. The ideal PV module model in (a) does not include the parasitic resistances R_s and R_p that account for the cell power loss due to the internal resistance of PV module. The single-diode model in (b) is the common used PV module, The double-diode model in (c) is reported in [9] and [12, 13]

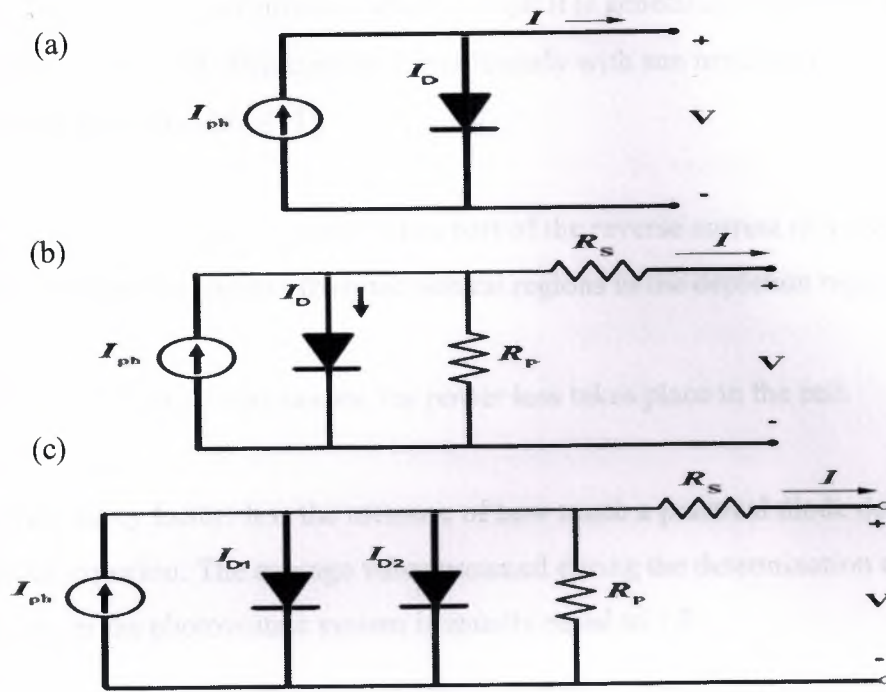


Figure 2.12 PV module equivalent circuit (a) ideal model, (b) single-diode model, (c) double-diode model [11].

The mathematical equations describing the three cases in Fig 2.12 are given respectively by:

The characteristic Equation for the PV cell is given by:

$$I = I_{pv} - I_{os} \left[e^{\frac{V+R_S I}{V_t a}} - 1 \right] \quad (2.4)$$

$$I = I_{pv} - I_{os} \left[e^{\frac{V+R_S I}{V_t a}} - 1 \right] - \frac{V+R_S I}{R_p} \quad (2.5)$$

$$I = I_{pv} - I_{os1} \left[e^{\frac{V+R_S I}{V_t a}} - 1 \right] - I_{os2} \left[e^{\frac{V+R_S I}{V_t a}} - 1 \right] - \frac{V+R_S I}{R_p} \quad (2.6)$$

Where;

I : The PV module terminal current (A)

V : The PV module terminal voltage (V)

I_{pv} (A): Light-generated Current or Photocurrent it is generated directly by an incident of sunlight on the PV cell. This current varies linearly with sun irradiation and depends on temperature given by [48], [11]:

I_{os} (A): Diode Saturation Current: It is a part of the reverse current in a diode caused by diffusion of minority carriers from the neutral regions in the depletion region.

R_s and R_p (Ω): internal resistances, the power loss takes place in the cell.

a : Diode ideality factor: It is the measure of how much a practical diode deviates from the ideal diode equation. The average value assumed during the determination of unknown parameters in the photovoltaic system is usually equal to 1.3.

$V_t = kT/q$: Junction thermal voltage: It is a characteristic voltage that relates the current flow in the p-n junction to the electrostatic potential across it.

Where,

K : Boltzmann's constant ($1.3806503 \times 10^{-23}$ J/K)

T : Nominal Temperature (298.15 K)

q : Charge of electron ($1.60217646 \times 10^{-19}$ C)

2.12 PV Cell Model Implementation

The implementation of the PV model was done by using MATLAB /Simulink package 2012 version , several PV models are presented in order to find the accurate, simplest, and best performance model which validated by using real time recorded data , the following models are implemented:

2.12.1 Model One

Mathematical equations are used in order to build the electric circuit equivalent to a PV cell this approach is presented by [21, 46, 50], this model is consisting of current source, which represents the photocurrent source in parallel with a diode. The output of the current

source is directly proportional to the light incident on the cell. The diode determines the I-V characteristics of the cell. The photocurrent depends on the cell temperature.

The series resistance R_s , gives more accuracy between the maximum power point and the open circuit voltage. R_p Shunt resistance in parallel with the diode, sets saturation currents. The model included temperature dependence of the photocurrent I_L and the saturation current of the diode I_{os} . A series resistance R_s was included, but not a shunt resistance. The circuit diagram of the solar cell is shown in Fig. 2.13. The equations that describe the I-V characteristics of the cell [20].

$$I = I_{pv} - I_{os} \left[e^{\frac{V+R_s I}{V_t a}} - 1 \right] \quad (2.7)$$

$$I_{pv} = I_{pv,nom} (1 + K_o (T - T_{nom})) \quad (2.8)$$

$$I_{pv,nom} = I_{sc,nom} \left(\frac{G}{G_{nom}} \right) \quad (2.9)$$

$$K_o = \frac{I_{sc,nom} - I_{sc,T}}{T_T - T_{nom}} \quad (2.10)$$

$$I_{os} = I_{os,nom} \left(\frac{T_T}{T_{nom}} \right)^{\frac{3}{n}} e^{\left(\frac{-E_g T_{nom}}{a V_t \left(\frac{1}{T_{nom}} - \frac{1}{T_T} \right)} \right)} \quad (2.11)$$

$$I_{os,nom} = \frac{I_{sc,nom}}{e^{\left(\frac{V_{oc,nom}}{a V_t T_T} \right)}} \quad (2.12)$$

$$R_s = -\frac{dV}{dV_{oc}} - \frac{1}{X_v} \quad (2.13)$$

$$X_v = I_{os,nom} \frac{1}{a V_t} e^{\left(\frac{V_{oc} T_{nom}}{a V_t T_{nom}} \right)} \quad (2.14)$$

All of the constants in the above equations were described in the previous section other parameters can be determined by examining the manufacturers' ratings of the PV array, and then the I-V curves of the array published or measured.

Where;

T_{nom} : Nominal temperature = 25° C.

T_2 : New Temperature required to calculate other variables.

G_{nom} : Nominal irradiance = 1000 W/m².

G : New Irradiance required to calculate other variables.

$I_{sc,nom}$: Short circuit current at nominal temperature.

T_T : Required simulation temperature.

$I_{sc,T}$: Short circuit current at required simulation temperature.

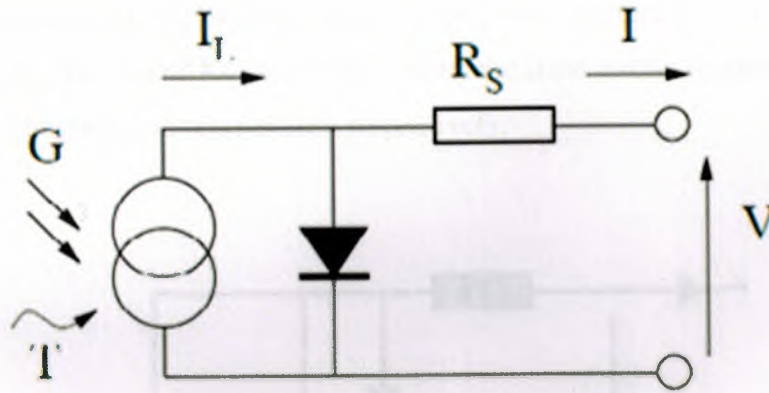


Figure 2.13 The circuit diagram of the PV model [21].

The implemented model is shown in Fig. 2.14 which consists of a MATLAB function used to calculate the photocurrent of PV cell connected in parallel with the diode, the total circuit was connected with resistance (R_s).

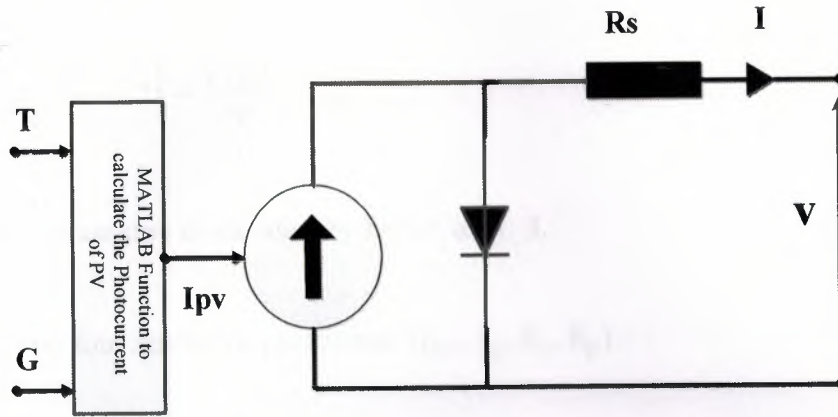


Figure 2.14 Implemented circuit diagram of PV model one.

2.12.2 Model Two

The proposed model designed according to [46, 48] this model are based on manufacturing data sheet were given with PV array . Some parameters are given such as open circuit voltage, short circuit current, maximum power, maximum current and maximum voltage, also K_i and K_v , which represents the short circuit current and open circuit voltage changing with temperature respectively.

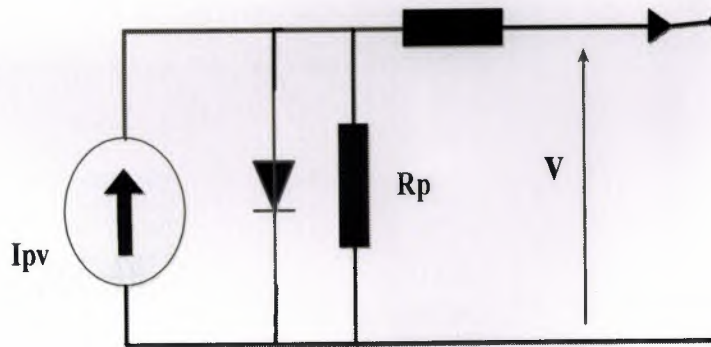


Figure 2.15 Implemented circuit diagram of PV model two.

There are five unknown parameters in the characteristic equation (2.15) of a single diode model which are, $(I_{pv}, I_{os}, a, R_s, R_p)$

$$I = I_{pv} - I_{os} \left[e^{\frac{V+R_s I}{V_t a}} - 1 \right] - \frac{V+R_s I}{R_p} \quad (2.15)$$

In this method, we assume diode ideality factor, $a = 1.3$.

Now, remain with four unknown parameters (I_{pv} , I_{os} , R_s , R_p)

I_{os} Can be calculated using equation (2.18), and (2.19)

I_{pv} Can be calculated using equations (2.16), (2.17)

$$I_{pv,n} = \frac{R_p + R_s}{R_p} * I_{s,n} \quad (2.16)$$

$$I_{pv} = (I_{pv,n} + K_i \Delta T) \frac{G}{G_n} \quad (2.17)$$

$$I_{os,n} = \frac{I_{sc,n}}{e^{\left(\frac{V_{oc,n}}{a V_t n}\right)^{-1}}} \quad (2.18)$$

$$I_{os} = I_{os,n} \left(\frac{T_n}{T}\right)^3 e^{\left[\frac{q E_g}{a K} \left(\frac{1}{T_n} - \frac{1}{T}\right)\right]} \quad (2.19)$$

There is one pair of R_s and R_p that's warranties ($P_{max,m} = P_{man,e}$) at maximum point condition.

$$P_{max,m} = V_{mp} \left[I_{pv} - I_{os} \left[e^{\frac{V_{mp} + R_s I_{mp}}{V_t a}} - 1 \right] - \frac{V_{mp} + R_s I_{mp}}{R_p} \right] = P_{max,e} \quad (2.20)$$

$$R_p = V_{mp} \left(\frac{V_{mp} + R_s I_{mp}}{V_{mp} I_{pv} - V_{mp} I_{os} \left[e^{\frac{V_{mp} + R_s I_{mp}}{V_t a}} \right] + V_{mp} I_{os} - P_{max,e}} \right) \quad (2.21)$$

In order to find the values of R_s and R_p , we need to do a certain number of iterations so that the peak value of power at maximum power-point, equals experimental MPP power, $P_{ma,e}$.

It can be easily done using a numerical method. It is required to choose proper initial conditions for these unknown parameters. They can be initialized with (0) and then slowly incremented. As mentioned earlier, parallel resistance can be approximated to the inverse of slope at maximum power point of the I-V curve. So, we can easily assume the initial condition for to be the negated inverse of the slope, Thus, we get

$$R_{p,min} = \frac{V_{mpp}}{I_{s,n} - I_{mpp}} \quad (2.22)$$

Previously, for simplicity, authors used to assume but since due to iterative updates and, the model developed can be further improved by [18].

$$I_{ph,n} = \frac{R_p - R_s}{R_p} I_{s,n} \quad (2.23)$$

Fig. 2.16 shows the algorithm that can be followed using MATLAB in order to find the unknown parameters of PV cell.

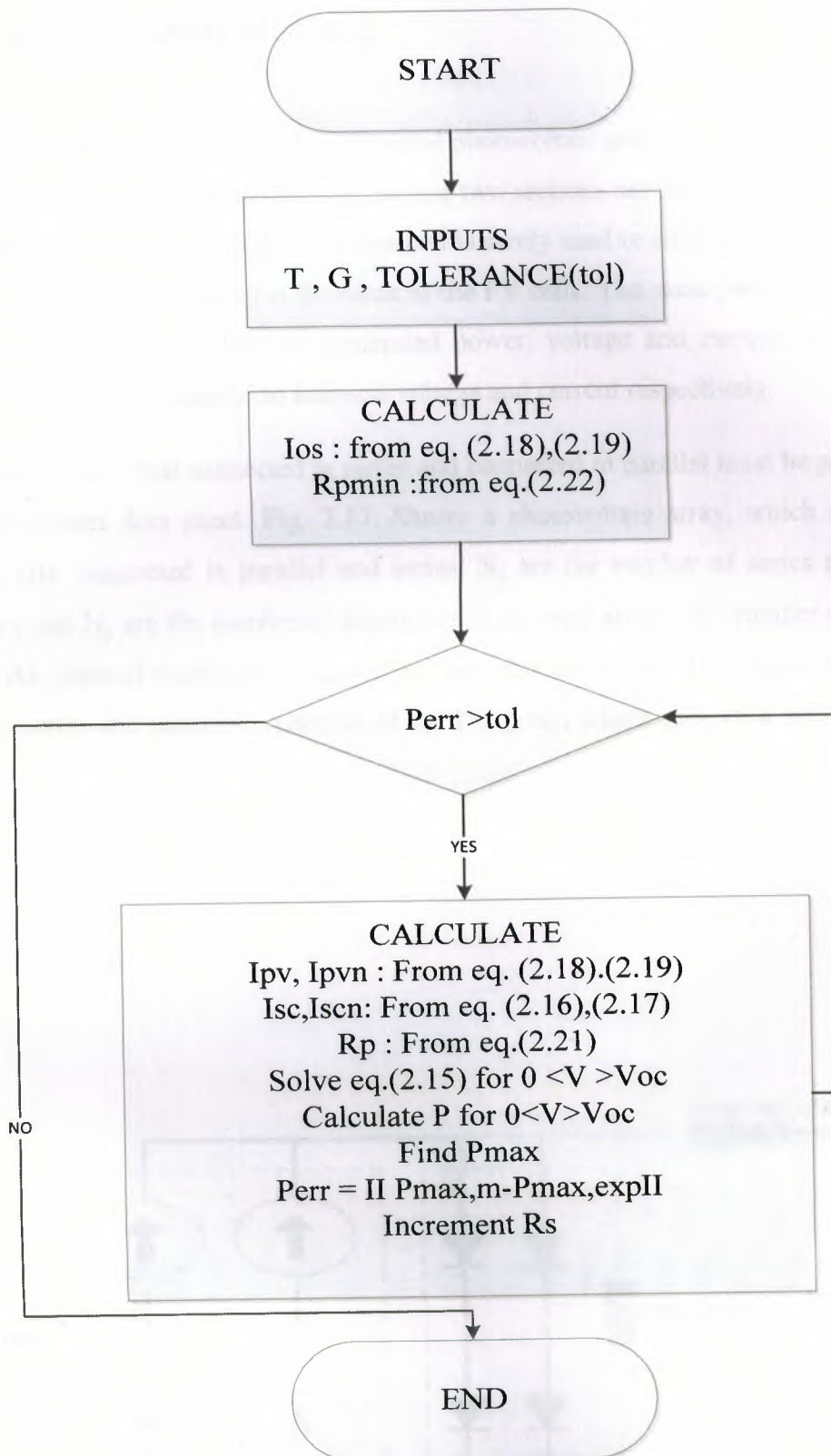


Figure 2.16 Flow chart of second modeling circuit.

2.13 Photovoltaic Array Modeling

The PV array consists of several interconnected photovoltaic cells (module) each cell has a specific characteristic, the calculation of the last two sections assumed that the cell has the same properties. In real life application one cell is rarely used in solar energy applications. The modeling of the solar array is the same as the PV cells. The same parameters from the data sheet are used. To obtain the generated power, voltage and current, the PV cells connected in series and parallel to increase voltage and current respectively.

The number of cells that connected in series and connected in parallel must be provided by the manufacturers data sheet. Fig. 2.17. Shows a photovoltaic array, which consists of multiple cells, connected in parallel and series. N_s are the number of series cells in the same array and N_p are the number of parallel cells in same array. The number of modules modifies the value of resistance in parallel and resistance in series. The value of equivalent resistance series and resistance parallel of the PV array, which presented by [50], which are:

$$R_{s,array} = \frac{N_s}{N_p} R_{s,cell} \quad (2.24)$$

$$R_{p,array} = \frac{N_s}{N_p} R_{p,cell} \quad (2.25)$$

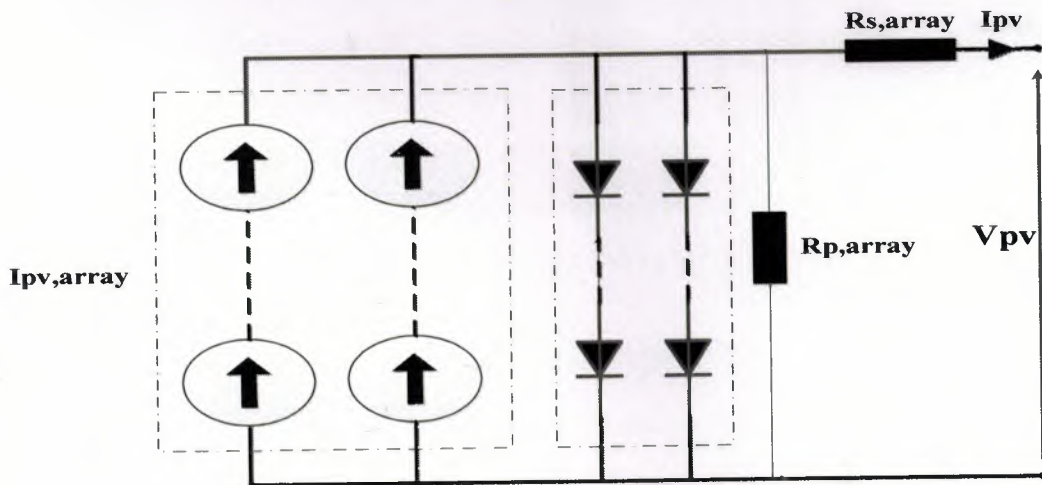


Figure 2.17 PV array composed of $N_s * N_p$ cells (module) [50].

The interconnection of many solar cells is affected by the photocurrent which is produced by the PV system, in addition to that, the voltage (V_{ph}) and current (I_{pv}) are also changed according to the new connection. The general equation of the photovoltaic current, which describes the current produced by PV, is changed as given below, as presented in [46].

$$I = I_{pv}N_p - I_{os}N_p \left[e^{\frac{V + R_s \left(\frac{N_s}{N_p} \right) I}{V_t a N_s}} - 1 \right] - \frac{V + R_s \left(\frac{N_s}{N_p} \right) I}{R_p \left(\frac{N_s}{N_p} \right)} \quad (2.26)$$

Where;

I_{os} , I_{pv} , V_t : are still having the same parameters used for a PV cell.

According to [46] Eq. 2.26. Is valid for any given array formed with identical modules. The two models, which were proposed in this thesis simulated by using the above equation to determine the photovoltaic current.

CHAPTER THREE

POWER ELECTRONIC DEVICES IN PV SYSTEMS

3.1 Overview

This chapter is composed of an introduction to the Power Electronics devices, DC/DC converter, types, topology, and detail description of MPPT algorithms, an introduction to inverters and controlling strategies are given in this chapter.

3.2 Power Electronics

Historically, power electronics have been predominantly employed in domestic, industrial, and information technology applications. However, due to advancements in power semiconductor and microelectronics technologies, their application in power systems has gained considerably more attention in the past two decades. Thus, power-electronic converters are increasingly utilized in power conditioning, compensation, and power filtering applications [51].

Power electronics have already found an important place in modern technology and has revolutionized control of power and energy. As the voltage and current ratings and switching characteristics of power semiconductor devices keep improving, the range of applications continues to expand in areas such as lamp controls, power supplies to motion control, factory automation, transportation, energy storage, multi megawatt industrial drives, and electric power transmission and distribution [52]. Power electronics systems are composed of simple electronic elements that are working to change the magnitude, frequency, and type of voltage and current according to the requirement of the users, some of power electronics devices work as [53]:

- AC/DC converters called rectifiers that convert input AC voltage, to DC with adjustment of output voltage and current.
- DC/AC converters called inverters that produce output ac voltage of controllable magnitude and frequency from input dc voltage.

- AC/AC converter called frequency converters and changers that establish the AC frequency, phase, magnitude, and shape.
- DC/DC converters called choppers that change DC voltage and current levels using the switching mode of semiconductor devices.

3.3 Power Electronics Converters

A power-electronic converter consists of a power circuit, which can be realized through a variety of configurations of power switches and passive components and a control protection system. The link between the two is through gating/switching signals and feedback control signals [53]. The power electronics converter system using primary electronic elements that are : resistors capacitors, transformers, inductors (choke coils), frames, etc., and basic classes of semiconductor devices [53]:

- Diodes, including Zener, optoelectronic and Schottky diodes, and diac
- Thyristors, such as silicon controlled rectifiers (SCR), Triacs, gate turn off (GTO), and metal oxide semiconductor controlled Thyristors (MCT).
- Transistors, particular bipolar junction (BJT), field effect (FET), and insulated bipolar (IGBT) transistors. A comparative diagram of power ratings and switching speeds of the controlled semiconductor electronic devices given in Fig. 3.1.

Fig. 3.2. Shows the symbols diagram of semiconductor devices used in power, which were diode, Thyristors, gate turn-off Thyristors (GTO), bipolar junction transistors, junction field effect transistors (GFET), metal-oxide semiconductor field effect transistors (MOSFET), and insulated gate bipolar transistors (IGBT).

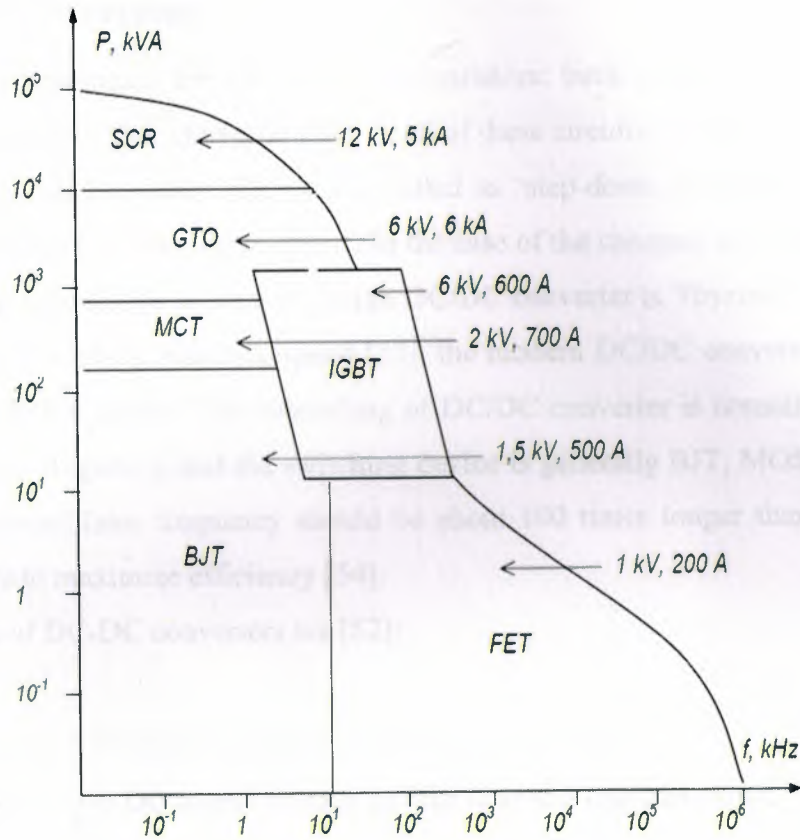


Figure 3.1 power ratings and switching speeds of the controlled semiconductor [53].

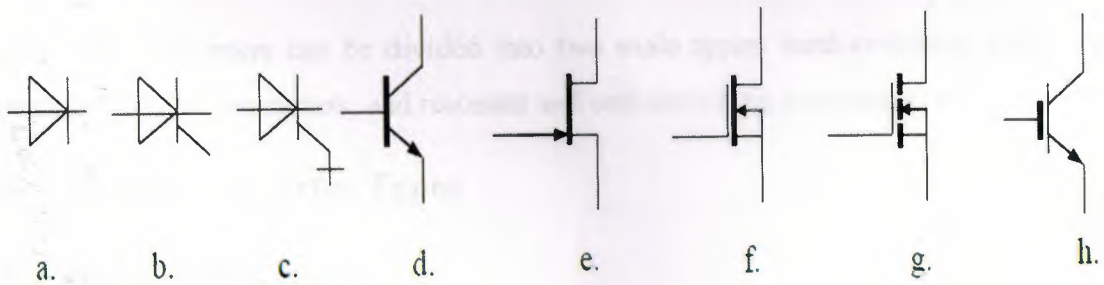


Figure 3.2 Semiconductor power electronics devices (a) diode, (b) Thyristors, (c) gate turn-off Thyristors (GTO), (d) bipolar junction transistors (BJT), (e) junction field effect transistors (JFET), (f-g) metal-oxide semiconductor field effect transistors (MOSFET), (h) insulated gate bipolar transistors (IGBT) [53].

3.4 DC/DC Converter

There are four topologies for the switching regulators: buck converter, boost converter, buck-boost converter, Cuk converter [54], in all of these circuits, a power device is used as a switch. The buck converter (DC/DC) is called as 'step-down chopper', whereas boost converter (DC/DC) is a 'step-up chopper'. In the case of the chopper, no buck-boost type is used [53]. The first device is used to design DC/DC converter is Thyristor, but due to the losses and low switching response speed [53], the modern DC/DC converter replaced the Thyristors by IGBT device. The controlling of DC/DC converter is normally achieved by PWM at a fixed frequency and the switching device is generally BJT, MOSFET or IGBT. The minimum oscillator frequency should be about 100 times longer than the transistor switching time to maximize efficiency [54].

The functions of DC-DC converters are [52]:

- To convert a DC input voltage into a DC output voltage;
- To regulate the DC output voltage against load and line variations;
- To reduce the AC voltage ripple on the DC output voltage below the required level;
- To provide isolation between the input source and the load (isolation is not always required);
- To protect the supplied system and the input source from electromagnetic interference (EMI); and
- To satisfy various international and national safety standards.

The DC/DC converters can be divided into two main types: hard-switching pulse width modulated (PWM) converters, and resonant and soft-switching converters [52]

3.5 DC/DC Converter Types

3.5.1 Buck Converters

Buck Converter is also known as the step down converter. It's typical application is to convert the input voltage into a lower output voltage [55], it is a switched-mode power supply that uses two switches, a transistor and a diode. A buck converter is shown in Fig. 3.3. The diode is used to allow the load current to flow through it, when the switch is turned off. If the switching device used is a Thyristor, this circuit is called as a step-down

chopper, as the output voltage is normally lower than the input voltage [53]. Fig. 3.4.

Shows the output voltage and load current of buck converter.

In [58] the buck converter has higher efficacy, lesser costs and can adjust to bear a higher amount of energy. The advantages and disadvantages (features) of buck converter can be summarized as given below [53]:

- Pulsed input current, requires input filter.
- Continuous output current results in lower output voltage ripple.
- Output voltage is always less than the input voltage.

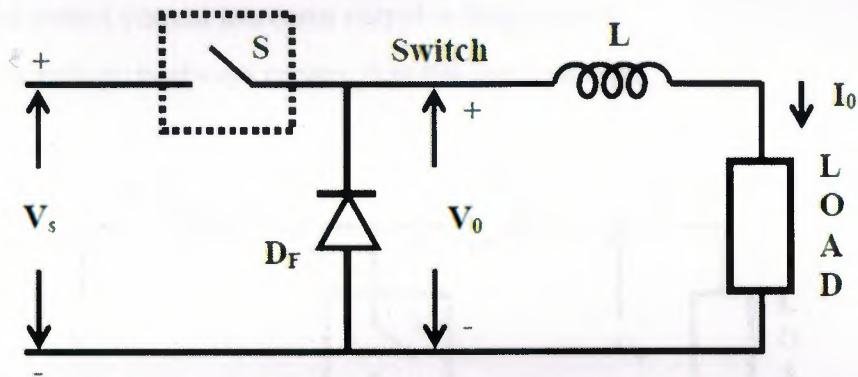


Figure 3.3 Buck converter circuit diagram [53].

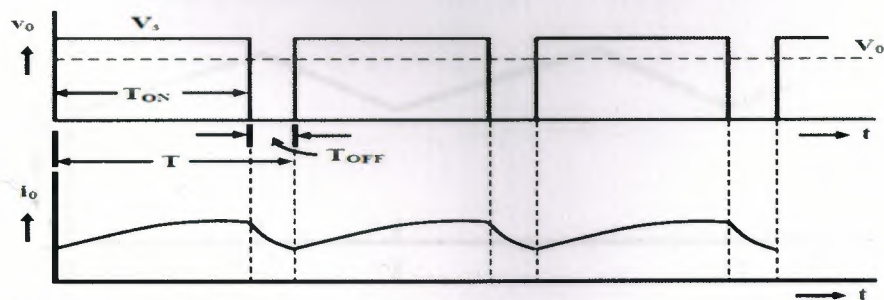


Figure 3.4 Output voltage and current waveforms [53].

3.5.2 Boost Converters

Boost Converter: also known as a step up converter. The typical application is increasing the output voltage [55]. A boost converter is shown in Fig. 3.5. For which a device belonging to transistor family is generally used [56]. The power source of boost converter can come from any suitable DC sources, such as batteries, solar panels, rectifiers and DC generators [54]. Fig. 3.6. Shows the load current of boost converter.

The advantages and disadvantages (features) of boost converter can be summarized as given below [53].

- Continuous input current, eliminates input filter.
- Pulsed output current increases output voltage ripple.
- Output voltage is always greater than the input voltage.

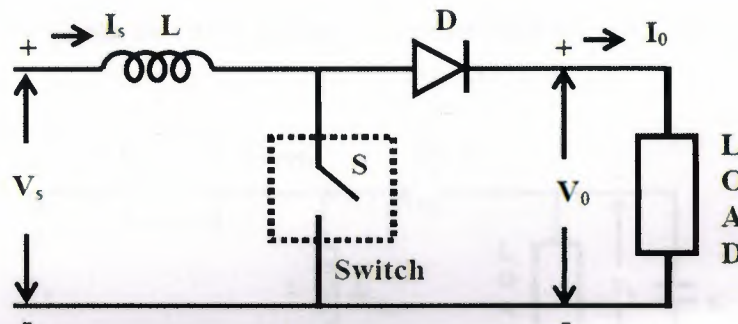


Figure 3.5 Boost converter circuit diagram [56].

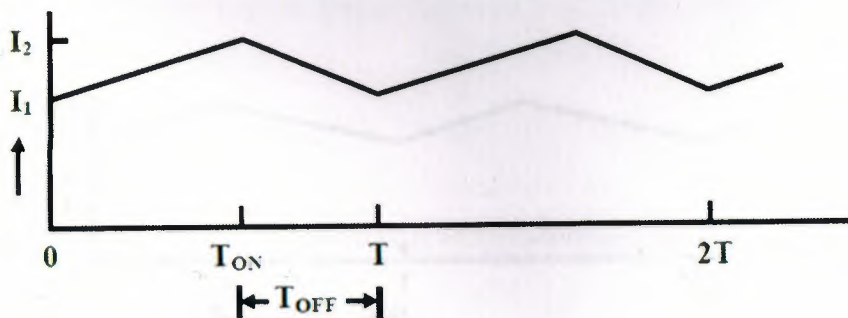


Figure 3.6 Waveforms of source current [56].

3.5.3 Buck-Boost Converters

A buck-boost converter is shown in Fig.3.7. The buck-boost converter is composed the properties of buck and boost converter, that has an output voltage magnitude that is either greater than or less than the input voltage magnitude [53]. The most common device used as a switch in a buck boost converter is a transistor, diode connected in series with the load and the inductor and capacitance connected in parallel [55]. The polarity of the output voltage is opposite to that of input voltage here. Fig. 3.8. Shows the load current of a buck boost converter.

The advantages and disadvantages (features) of buck-boost converter can be summarized as given below [53].

- Pulsed input current, requires input filter.
- Pulsed output current increases output voltage ripple.
- Output voltage can be either greater or smaller than the input voltage.

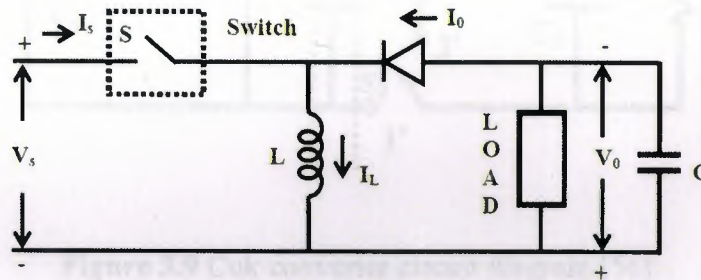


Figure 3.7 Buck-boost converter circuit diagram [56].

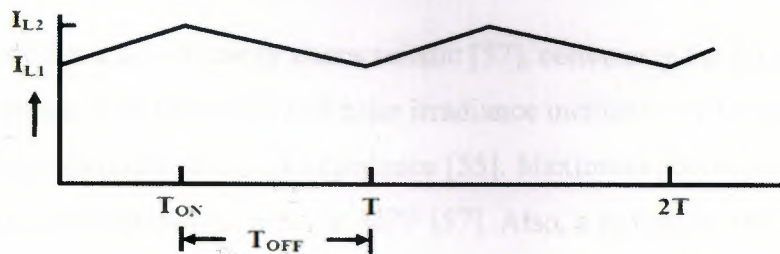


Figure 3.8 Inductor current (I_L) waveform [56].

3.5.4 Cuk converter

The Cuk converter shown in Fig. 3.9. Shared the buck-boost converter in the operation and the polarity of output voltage, there is one difference between Cuk converters is it uses a capacitor as its main energy-storage component, unlike most other types of converters, which use an inductor [55].

- Cuk converter is one such converter. It has the following advantages [53].
- Continuous input current.
- Continuous output current.
- Output voltage can be either greater or less than the input voltage.

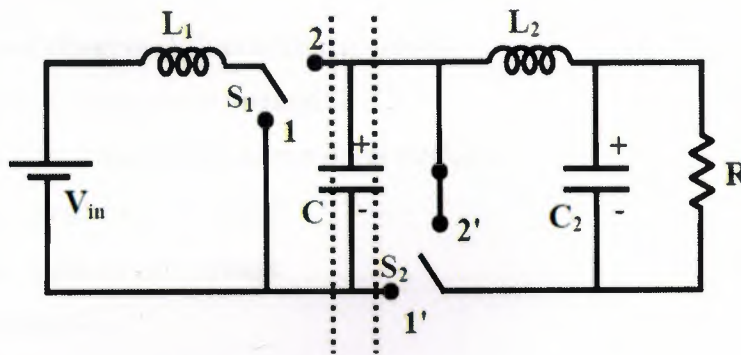


Figure 3.9 Cuk converter circuit diagram [56].

3.6 Maximum power point Tracking controller and algorithm

The Photovoltaic has a non-linearity characteristic [57], conversely the power output of the PV module changes, with the amount of solar irradiance incident on PV system, also with the variation of temperature and load impedance [55]. Maximum power point controller allows operating the photovoltaic array at MPP [57]. Also, a typical solar panel converts only 30 to 40 percent of the incident solar irradiation into electrical energy, and according to [57] "for single PV cell, extracting the maximum power is relatively easy simple algorithms can be applied to search the right operating point on the I-V curve of the

photovoltaic cell when building a photovoltaic generator by connecting photovoltaic modules in series to boost the voltage of the generator, certain difficulties arise, for example, multiple maximum power points can occur. Multiple maximum power points cannot be detected by using simple maximum power point tracking techniques” MPPT used the Maximum Power Transfer theorem; the power output of a circuit is maximum when the Thevenin impedance of the circuit (source impedance) matches with the load impedance [54], [58]. From the above description it is clear that the use of MPPT in PV system cannot be overlooked, many MPPT algorithms used by researchers in order to find the best MPPT algorithms, with the fact that each algorithm has Pros and cons.

3.6.1 Different MPPT techniques

There are different techniques used to track the maximum power point. Some of the most common techniques are [54], [55]:

1. Perturb and Observe (hill climbing method).
2. Incremental Conductance method (INC).
3. Voltage control maximum power point tracker.
4. Fractional short circuit current.
5. Fractional open circuit voltage
6. Neural networks
7. Fuzzy logic
8. Parasitic capacitances
9. Current control maximum power point tracker

The presented list of algorithms starts from simple complexity and the cost of implementation goes on increasing which may be suitable for a highly complicated system. This is the reason that Perturb and Observe and Incremental Conductance method are the most widely used algorithms. So due to the simplicity of implementation we have chosen the two algorithms P&O and INC algorithms for our study among the presented list [54].

3.6.2 Perturb and observe

Perturbation and Observation method also known as Hill Climbing method [55], [59] is one of the most popular algorithms. As the name implies the method will perturb the system by either increasing or decreasing the array's operating voltage point and comparing the result to the one obtained in the previous perturbation cycle. If the perturbation leads to an increase or decrease in array power, the subsequent perturbation is made in the same or opposite direction [59].

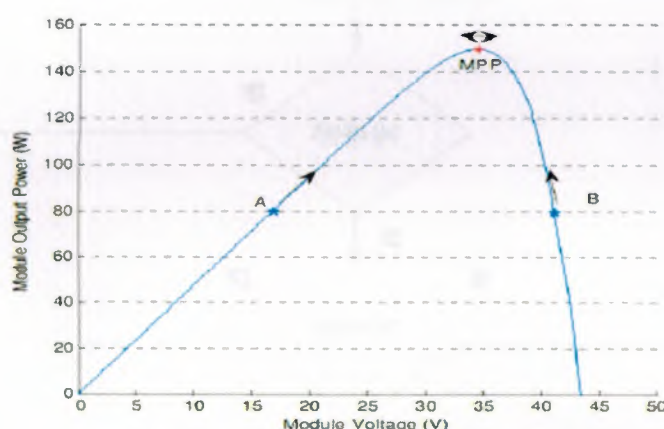


Figure 3.10 P-V curve showing MPP and operating points A and B [54].

Figure 3.10 shows the plot of module output power versus module voltage for a solar panel at a given irradiation. The point marked as MPP is the Maximum Power Point, the theoretical maximum output obtained from the PV panel.

Consider A and B as two operating points. As shown in the Fig.3.10. The point A is on the left hand side of the MPP. Therefore, we can move towards the MPP by providing a positive perturbation to the voltage. On the other hand, point B is on the right hand side of the MPP. When we give a positive perturbation, the value of (P) becomes negative, thus it is imperative to change the direction of perturbation to achieve MPP [59]. The flowchart for the P&O algorithm is shown in Fig. 3.11.

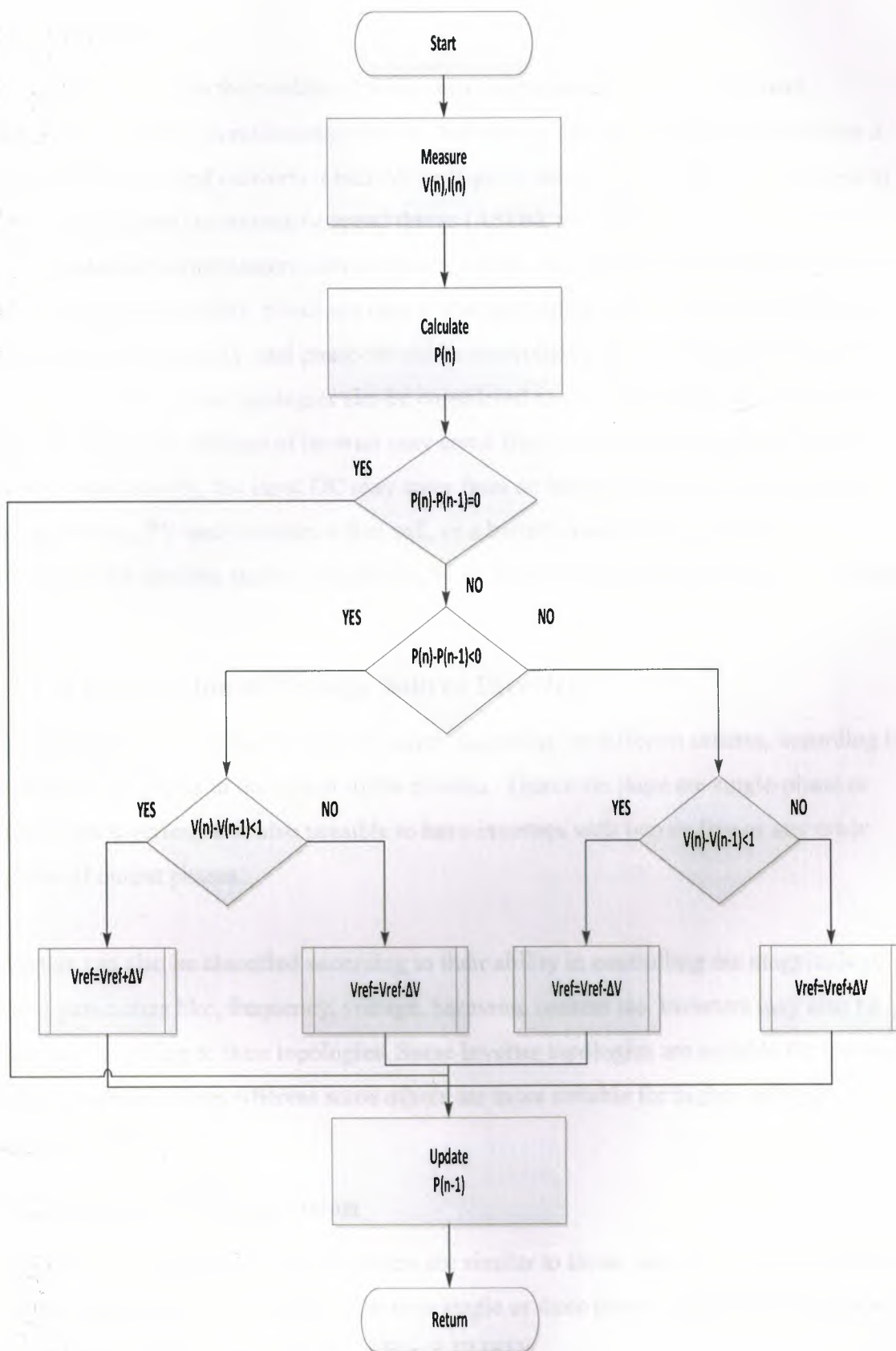


Figure 3.11 Flow chart of the P&O algorithm.

3.7 Inverter

The word 'inverter' in the context of power-electronics denotes a class of power conversion (or power conditioning) circuits that operates from a DC voltage source or a DC current source and converts it into AC voltage or current [56]. These are the types of waveforms required in adjustable speed drives (ASDs), uninterruptible power supplies (UPS), static var compensators, active filters, flexible AC transmission systems (FACTS), and voltage compensators, which are only a few applications. For sinusoidal AC outputs, the magnitude, frequency, and phase should be controllable. According to the type of AC output waveform, these topologies can be considered as voltage source inverters (VSIs) [60]. The input DC voltage of inverter may come from the rectified output of a power supply. Alternatively, the input DC may enter from an independent source, such as a DC voltage source, PV array system, a fuel cell, or a battery. Generally, controlled semiconductor devices, such as transistors, SCR, and GTO Thyristors are used in inverters [53].

3.7.1 Classification of Voltage Source Inverters

The classification of voltage source inverters depending on different criteria, according to the number of phases in the output of the inverter. Therefore, there are single-phase or three-phase inverters. It is also possible to have inverters with two or five or any other number of output phases.

Inverters can also be classified according to their ability in controlling the magnitude of output parameters like, frequency, voltage, harmonic content etc. Inverters may also be classified according to their topologies. Some inverter topologies are suitable for low and medium voltage ratings whereas some others are more suitable for higher voltage applications [53, 60].

3.7.2 Inverter Configuration

The circuit arrangements used in inverters are similar to those used in the rectifiers. The inverter applications are however limited to single or three phase circuits. There are six types of configuration in common use Fig. 3.12 [61]:

- Chopper type.

- Center Tapped load.
- Single phase bridge.
- Three phase bridge.
- Center tapped load.

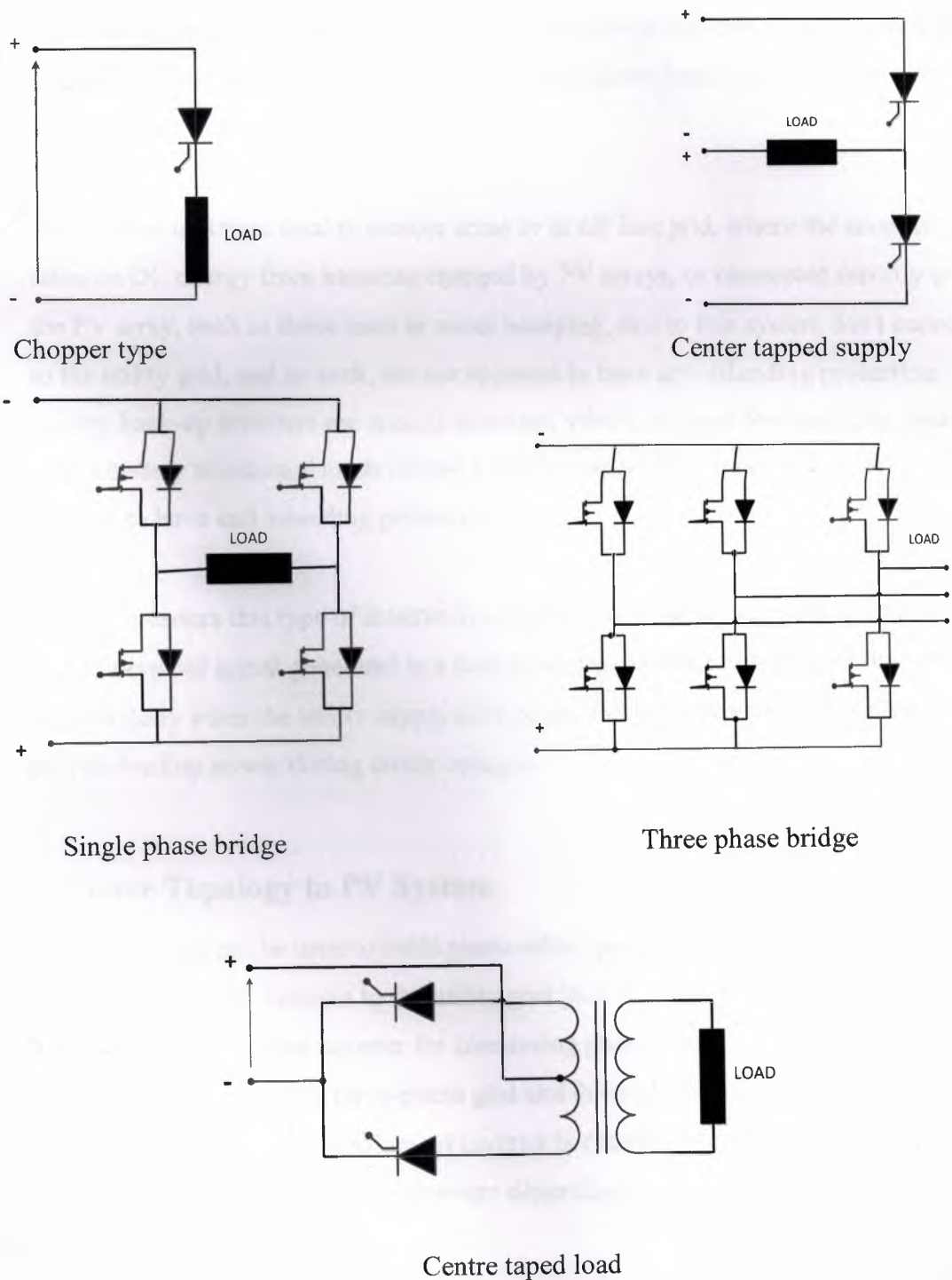


Figure 3.12 Inverter configuration [63]

3.7.3 Solar Inverters

Solar inverter is one of most efficient inverters, used to change the DC voltage to AC voltage, the size and capacity of this type of inverters are varying according to supply power requirement. Solar inverter may use for domestic or industrial, and for large scale such as solar energy plant, The solar energy is collected during the daytime and used at the time of need after being converted into electrical energy. Some basic types of solar inverters are:

- Stand-alone inverters used in remote areas or in off line grid, where the inverter takes its DC energy from batteries charged by PV arrays, or connected directly to the PV array, such as those used in water pumping, due to this system don't connect to the utility grid, and as such, are not required to have anti-islanding protection. Battery back-up inverters are special inverters, which are used for supplying energy from a battery to selected loads during a utility outage. This type of inverter required to have anti-islanding protection.
- Grid-tie inverters this type of inverter is connected and supplying with the utility grid, the type of signal generated is a sine wave, this inverter designed to shut down automatically when the utility supply shut down, for safety reasons. They do not provide backup power during utility outages.

3.7.4 Inverter Topology in PV System

Different topology that can be used to build photovoltaic generator system and technologies to connect PV systems to the utility grid [62]. Various inverter configurations are used. There are single-phase inverter for connecting photovoltaic modules to a single-phase grid or more of them to the three-phase grid and three-phase inverter for connecting to the three-phase grid [63]. The topology of inverter is centralized inverters, string inverters, AC modules and multi-string inverters depending on the modularity of the system [63].

- Multi string inverter

In this topology, “multiple PV module or string is connected to a dedicated DC/DC converter that is connected to a common DC/AC inverter.”[64]. Each PV string has its own boost converter and MPPT. Each PV operates at MPP. Fig. 3.13. (a) represents the multi string inverter and can be noted that each DC/DC converters typically link with each other by means of DC bus via an inverter.

The advantage with multistring inverter is its ability to add an extra PV module to the bus if more power is needed in the future. In case of failure of one PV string, the PV system still able to operate with the remaining PV [63, 64].

– Centralized inverters

Central inverter topology or common name is a single stage photovoltaic system. In this topology, the PV system includes a series-parallel connection arrangement, which is connected to a single inverter DC/AC for the higher amount of power, which is connected to the grid or the load. Single stage photovoltaic is shown in Fig. 3.13. (b), this type of DC/AC inverter that must include the MPPT algorithm and DC/DC converter in order to extract Maximum power from PV [63],[64].

– Micro inverter

The micro inverter is a small inverter rated to handle the output of a single PV array or a small group of PV's , these types of micro-inverters are typically rated between 200 and 230 W. The output from several micro-inverters are combined and often connected to the utility grid. Each micro-inverter harvests optimum power by performing MPPT for its connected panel. The micro inverter is simple to design and stock, they can be used with any size of the PV array and a wide variety of panel types [67]. Micro inverter is shown in Fig. 3.13. (c).

– String inverter

String inverter or so called two stages PV system have the following drawbacks of lower effectiveness, higher count of parts, lower level of reliability, bigger size and higher cost. This topology is mostly used due to its simplicity [63]. The two-stage PV system photovoltaic is shown in Fig. 3.13. (d).

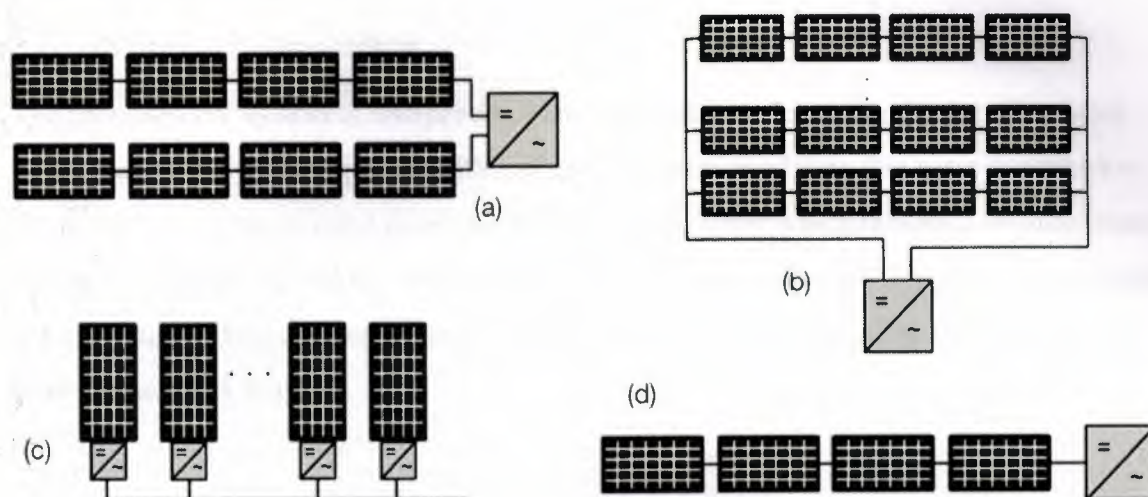


Figure 3. 13 PV plant different connecting topology; (a) Multi string inverter, (b) Central inverter, (c) Micro inverter, (d) String inverter [65].

AC module is an integrated system in which only one photovoltaic module is connected through interfacing equipment to the grid. AC modules offer very modular solution to build a photovoltaic system. There are very little power losses due to MPPT because every module has its own tracker.

The problem is that inverters have high price per watt ratio. AC modules are very suitable for mass production which can lead to low manufacturing costs in the future. AC module is illustrated in Fig. 4.14 [65].

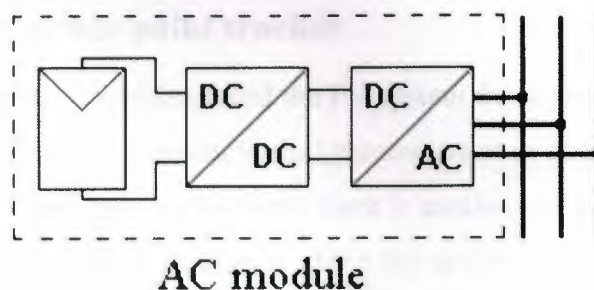


Figure 3.14 AC module configuration of a photovoltaic generator [6].

3.8 Proposed Simulation

The proposed PV system is composed of three phases in order to build a complete solar power generator; the first phase is PV cell and PV array modeling that were described in the previous chapter, second phase is the DC/DC converter which integrate the maximum power point tracking, and the third phase is DC/AC inverter design. The designed circuits are validated by real time recording for small or large-scale system Fig. 3.15. Shows the three phase block diagram.

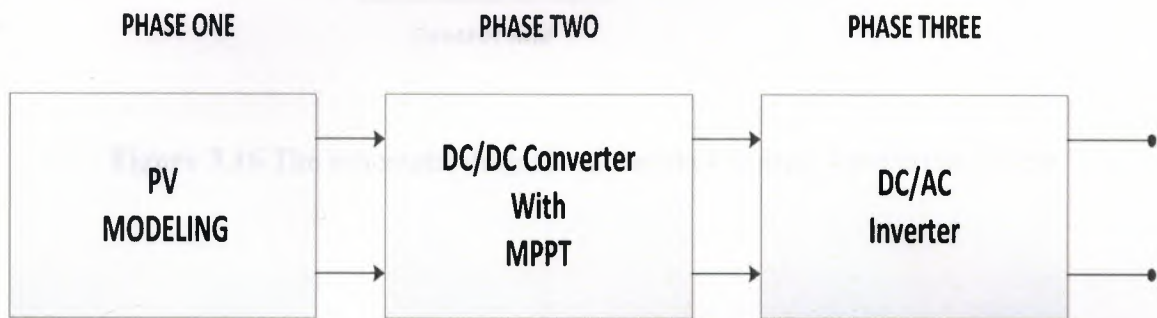


Figure 3.15 The proposed design phases.

3.8.1 PHASE TWO: MPPT and DC/DC Converter

3.8.1.1 Maximum power point tracker

One of the most important problems faced the PV system designers is changing the produced power with loads and climatological parameters such as irradiance, and temperature, in addition to these parameters , there is another parameter which is changing the load characteristic. All these parameters affect the produced power in a PV array. Therefore, the maximum power point tracker is necessary to draw the maximum power from the PV module. The MPPT algorithm is controlling the DC/DC converter by using the PWM to change the duty cycle point of operation of the module to pulses which control

the DC/DC converter. Fig. 3.16 shows the general diagram of the proposed DC/DC converter and Fig. 3.17 presents the internal circuit of MPPT system.

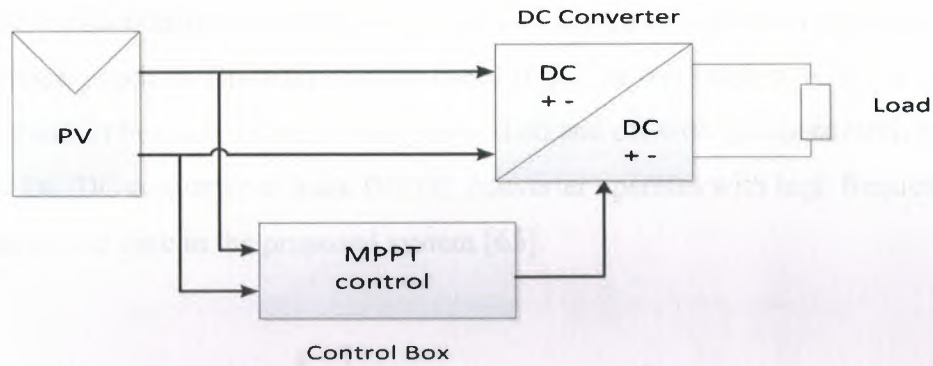


Figure 3.16 The schematic diagram of the photovoltaic simulation system.

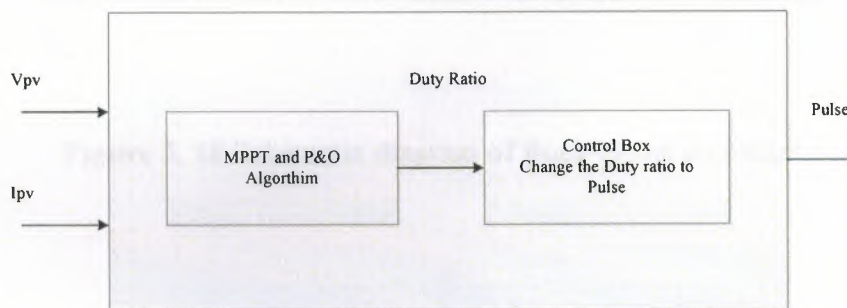


Figure 3.17 Block Diagram of MPPT control box.

3.8.1.2 Buck Boost Converter

A Buck Boost type DC/DC converter is proposed as the first stage with regulated output inductor current, The Buck Boost converter circuit consist of MOSFET switch Q, inductor L, diode D, filter capacitor C. As shown in Fig. 3.18. Since the circuit runs either in boost

or buck mode, its first stage can be very efficient if the low conduction voltage drop power MOSFET and ultra-fast reverse recovery diode is used.

For the second stage, because the unfolding circuit only operates at the line frequency and switches at zero voltage and current, the switching loss can be omitted. The only loss is due to the conduction voltage drop, which can be minimized with the use of low on drop power devices, such as Thyristor or slow-speed IGBT. In this version, IGBT is used in the unfolding circuit because it can be easily turned on and off with gating control, since only the boost DC/DC converter or buck DC/DC converter operates with high frequency switching all the time in the proposed system [65].

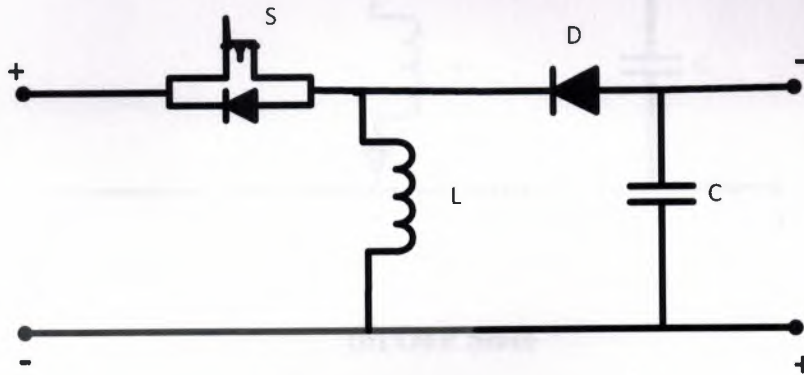
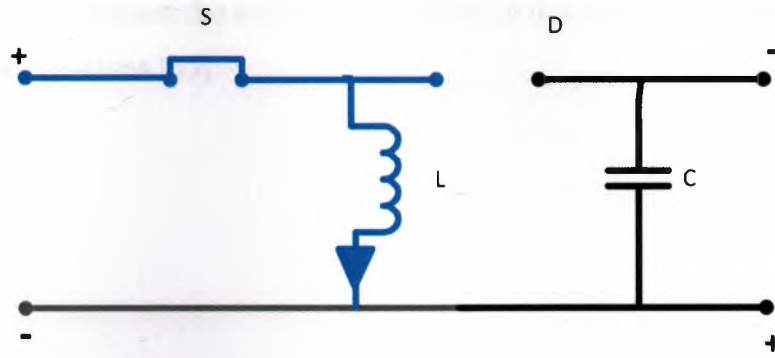


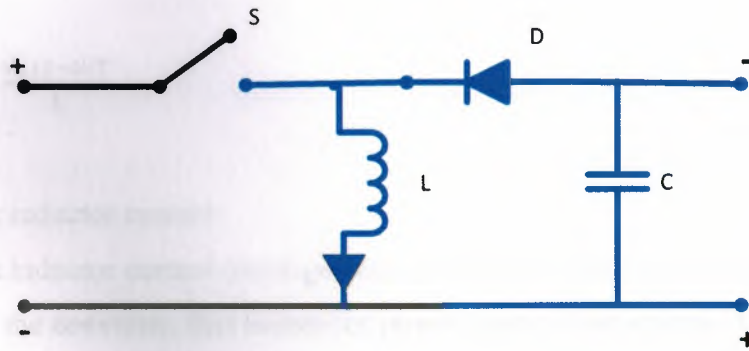
Figure 3. 18 Schematic diagram of Buck-Boost converter

– Operation Principle

When the switch is turned-on, Fig. 3.19 the input voltage source supplies current to the inductor, and the capacitor supplies current to the output load. When the switch is opened, the inductor supplies current to the load via the diode D, the Energy is stored in inductor when the switch is close and transferred to load when the switch is opened [65].



(a) On State



(b) OFF State

Figure 3.19 The two operating states of a buck–boost converter.

The Fig. 3.19 (a) shows the circuit diagram of buck- boost converter when the switch is closed, these equations describe the circuit [65]:

$$V_L = V_d = L \frac{di}{dt} \quad (3.1)$$

$$\frac{di_L}{dt} = \frac{V_d}{L} \quad (3.2)$$

$$\frac{\Delta i_L}{\Delta t} = \frac{\Delta i_L}{DT} = \frac{V_d}{L} \quad (3.3)$$

$$(\Delta i_L)_{closed} = \frac{V_d DT}{L} \quad (3.4)$$

The off state condition when the switch is turned off, in this case the system can be described by the equations [65].

$$V_L = V_o = L \frac{di_L}{dt} \quad (3.5)$$

$$\frac{di_L}{dt} = \frac{V_o}{L} \quad (3.6)$$

$$\frac{\Delta i_L}{\Delta t} = \frac{\Delta i_L}{(1-D)T} = \frac{V_o}{L} \quad (3.7)$$

$$(\Delta i_L)_{opened} = \frac{V_o (1-D)T}{L} \quad (3.8)$$

– Average inductor current

To calculate the inductor current (average value), assuming that there is no power consumption in the converter, that means the power supply from source is completely transferred to the load [65].

$$p_o = p_s \quad (3.9)$$

$$\frac{V_o^2}{R} = V_d I_s \quad (3.10)$$

But the average source current is related to the average inductor current as:

$$I_s = I_L D \quad (3.11)$$

$$\frac{V_o^2}{R} = V_d I_L D \quad (3.12)$$

Substituting for V_o ,

$$I_L = \frac{V_o^2}{V_d R D} = \frac{p_o}{V_d D} = \frac{V_o^2}{R(1-D)^2} \quad (3.13)$$

Maximum and Minimum inductor current can be calculated by:

$$I_{max} = I_L + \frac{\Delta i_L}{2} = \frac{V_d D}{R(1-D)^2} + \frac{V_d DT}{2L} \quad (3.14)$$

$$I_{min} = I_L - \frac{\Delta i_L}{2} = \frac{V_d D}{R(1-D)^2} - \frac{V_d DT}{2L} \quad (3.15)$$

The Buck boost converter has two operating modes, which are, continuous mode and discontinuous the two modes are described below:

- Continuous mode

In this thesis, the operation of buck boost converter is a continuous mode the Eq. (3.16) shows the relationship between load current and source voltage. If the current through the inductor L never fall to zero during a commutation cycle, the converter is said to operate in continuous mode. The current and voltage waveforms in an ideal converter can be seen in Fig. 3.20.

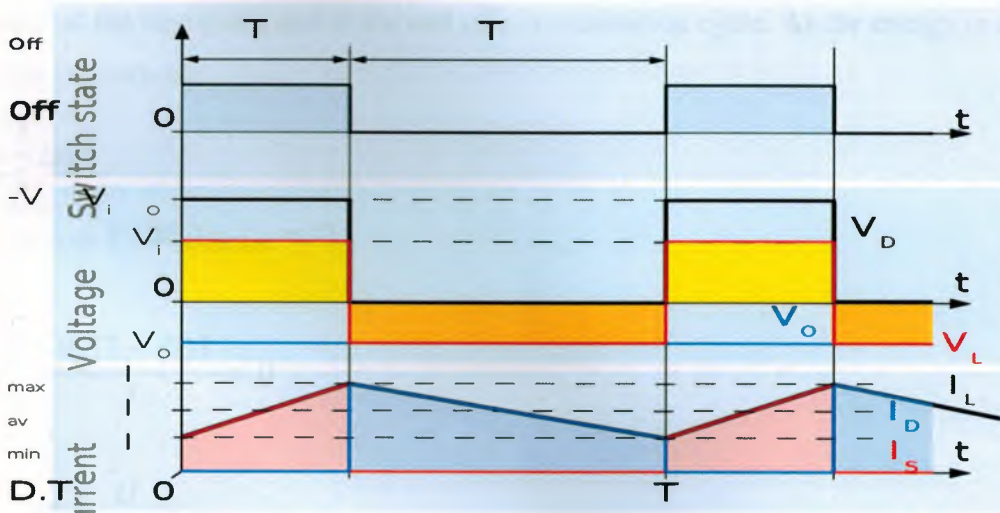


Figure 3.20 Waveforms of current and voltage in a buck-boost converter operating in continuous mode [65].

When $t=0$ to $t=DT$, the switch is on, the rate of change in the inductor current (i_L) is given by:

$$\frac{di_L}{dt} = \frac{V_d}{L} \quad (3.16)$$

$$(\Delta i_L)_{opened} = \int_0^{DT} di_L = \int_0^{DT} \frac{V_d}{L} dt = \frac{V_d DT}{L} \quad (3.17)$$

D is the duty cycle. It represents the fraction of the commutation period T during which the switch is on. Therefore D ranges between 0 (S is never on) and 1 (S is always on).

During the Off state, the switch S is open, so the inductor current flows through the load. If we assume zero voltage drops in the diode, and a capacitor large enough for its voltage to remain constant.

Therefore, the variation of i_L during the Off-period is:

$$(\Delta i_L)_{off} = \int_0^{(1-D)T} di_L = \int_0^{(1-D)T} \frac{V_d}{L} dt = \frac{V_d(1-D)T}{L} \quad (3.18)$$

At Steady state operation, the amount of energy stored in each of its components has to be the same at the beginning and at the end of a commutation cycle. As the energy in an inductor is given by:

$$E = \frac{1}{2} Li_L^2 \quad (3.19)$$

$$(\Delta i_L)_{opened} + (\Delta i_L)_{closed} = 0 \quad (3.20)$$

$$\frac{V_d DT}{L} + \frac{V_o (1-D)T}{L} = 0 \quad (3.21)$$

$$V_o = -V_d \left(\frac{D}{1-D} \right) \quad (3.22)$$

The Output voltage of buck- boost converter is opposite to the input in polarity. Finally,

$$D = \frac{V_d}{V_d + V_o} \quad (3.23)$$

The output of a buck-boost converter it will be higher or lower than the input, which mainly depended upon the value of D.

If $D > 0.5$, output is higher than the input

If $D < 0.5$, output is lower input

Apart from the polarity, this converter is either step-up (as a boost converter) or step-down (as a buck converter). This is why it is referred to as a buck-boost converter

– Discontinuous mode

In some cases, the amount of energy required by the load is small enough to be transferred at a time smaller than the whole commutation period. In this case, the current through the inductor falls to zero during part of the period. The only difference in the principle described above is that the inductor is completely discharged at the end of the commutation cycle as shown in the Fig. 3.21. Although slight, the difference has a strong effect on the output voltage equation. It can be calculated as follows:

As the inductor current at the beginning of the cycle is zero, its maximum value i_{Lmax} (at $t=DT$) is

$$i_{Lmax} = \frac{V_d DT}{2L} \quad (3.24)$$

During the off-period, i_L falls to zero after $\delta.T$:

$$i_{Lmax} + \frac{V_d \delta T}{2L} = 0 \quad (3.25)$$

Using the two previous equations, δ is:

$$\delta = -\frac{V_d D}{V_o} \quad (3.26)$$

The load current I_o is equal to the average diode current (I_D). As can be seen in Fig. 3.21.

The diode current is equal to the inductor current during the off-state. Therefore, the output current can be written as:

$$I_o = I_D = \frac{i_{Lmax}}{2} \delta \quad (3.27)$$

Replacing i_{Lmax} and δ by their respective expressions yields:

$$I_o = \frac{V_d DT}{2L} \frac{V_d D}{V_o} = -\frac{V_d^2 D^2 T}{2LV_o} \quad (3.26)$$

Therefore, the output voltage gain can be written as:

$$\frac{V_o}{V_d} = -\frac{V_d^2 D^2 T}{2LI_o} \quad (3.27)$$

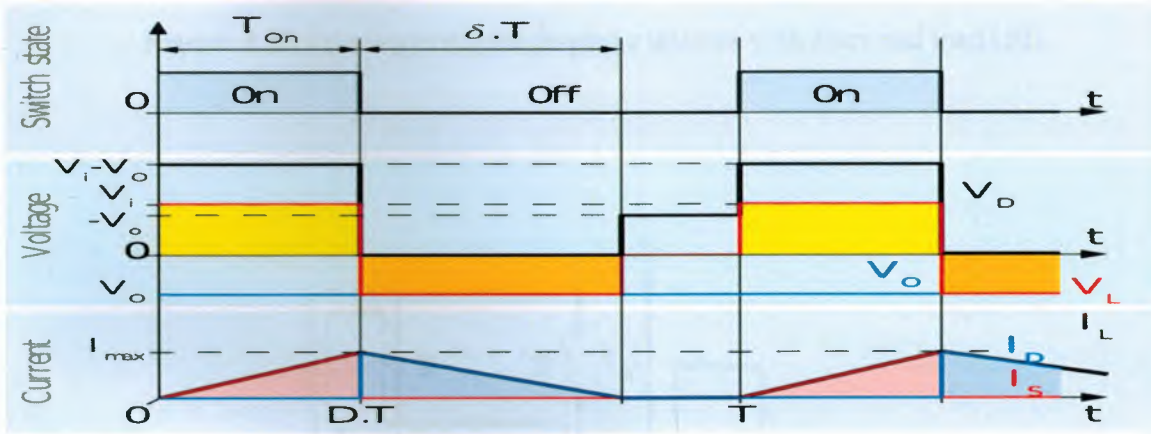


Figure 3.21 Waveforms of current and voltage in a buck–boost converter operating in discontinuous mode [65].

3.8.2 PHASE THREE: DC/AC Inverter

In photovoltaic system, the DC/AC inverter is a single phase bridge connected inverter shown in Fig. 3.22. Used to convert the power of the source by switching the DC input voltage to generate an AC voltage at the output. The single-phase bridge inverter has four

switches that turn on and off to get a sinusoidal output. To generate an AC waveform in single-phase inverter, the switches S1, S2 should be ON and S3, S4 should be OFF for period t_1 and t_2 as shown in Fig. 3.23. For that period, the output is a positive voltage for period t_2 to t_3 in Fig. 3.24. The switches S3, S4 are on and S1 and S2 are off to obtain negative voltage [50].

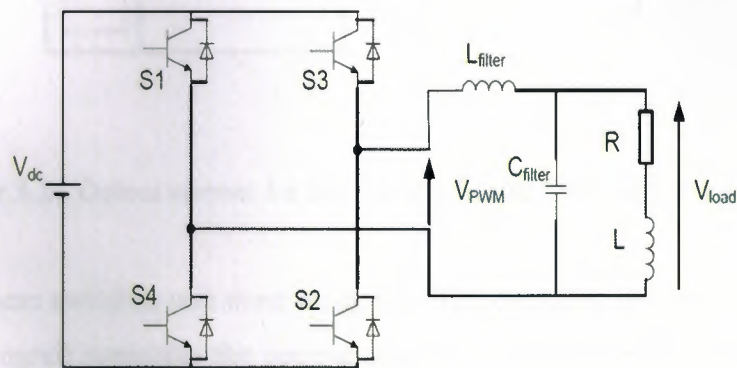


Figure 3.22 Topology of a single-phase inverter with filter and load [50].

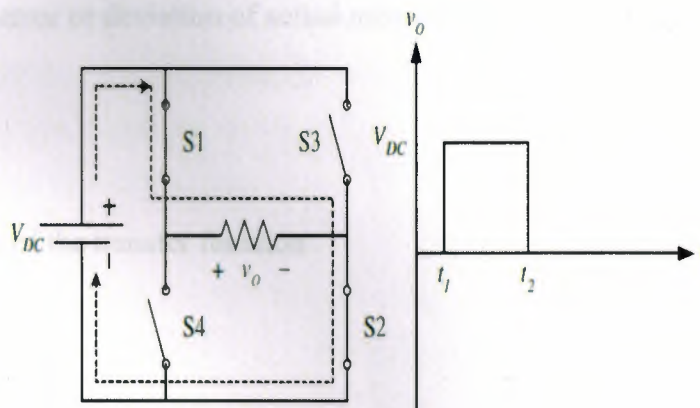


Figure 3.23 Output current for S1, S2 ON; S3, S4 OFF for $t_1 < t < t_2$ [50].

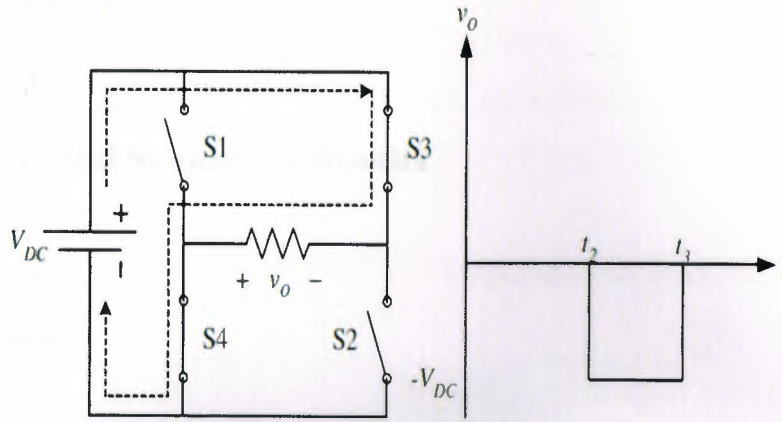


Figure 3.24 Output current for S3, S4 ON; S1, S2 OFF for $t_2 < t < t_3$ [50].

The control of these switches was done using the PID controller approach specially PI (proportional-integral) controller the general equations which were described this control system are given below:

The controller output given by

$$K_p \Delta + K_i \int \Delta dt \quad (3.28)$$

Where; Δ is the error or deviation of actual measured value (PV) from the set point (SP).

$$\Delta = SP - PV \quad (3.29)$$

The general form of the transfer function

$$G_c = \frac{V_o(s)}{V_i(s)} = K_p + \frac{K_i}{s} \quad (3.30)$$

$$G_c = K_p \left(1 + \frac{1}{T_i s}\right) \quad (3.31)$$

$$\text{Where } T_i = \frac{K_p}{K_i}$$

$$G_c = K_p \frac{T_i s + 1}{T_i s} \quad (3.37)$$

CHAPTER FOUR

Experimental and Simulation Results

4.1 Overview

This chapter is composed of two main sections, section one consists of experimental work and section two of simulation work which includes, solar array models where two models are given. Validation of implemented models is presented in order to find suitable circuit, also two MPPT algorithms are simulated to achieve maximum output power in all operating conditions, and DC/DC converter is given and simulated. In addition, DC/AC converters are simulated and the output waveforms are given. Finally, the last section will be the results and discussion.

4.2 Experimental Work

The experimental work is based on real data, which were recorded at outdoor conditions. The data of PV system were taken during a one year period (three to four times) per week, and (twelve to thirteen times) per month in Koya city (KRG of IRAQ) . The following equipments are used in recorded data.

- Two Solar Cell panel PV (NT 111 SHARP), the short circuit current is (2.7 A), open circuit voltage is (21.6 V), max. power is (43 W), and module area is (0.504 m²). It consists of (4*9) single silicon crystal cells Fig. 4.1 shows the two panels which used in the experimental work.
- Variable resistance model (Box 1051) from Time Electronic LTD. This variable resistance will be used as load to calculate the electrical power supply by the PV system, the load resistance changed between (10-190) Ω . Fig. 4.2 shows the variable resistance used in the experimental work.

- Explorer GLX (real time recorder) Real-time graphing and calculations from Floating Point Processor even instant calculations on live data as it is collected, this equipment used for monitoring and record the ambient and panel temperature
- Digital Multimeter used to calculate the current pass through load resistance, and voltage across the resistance.
- Two Thermo coupled to measure the ambient and back of panel temperatures.

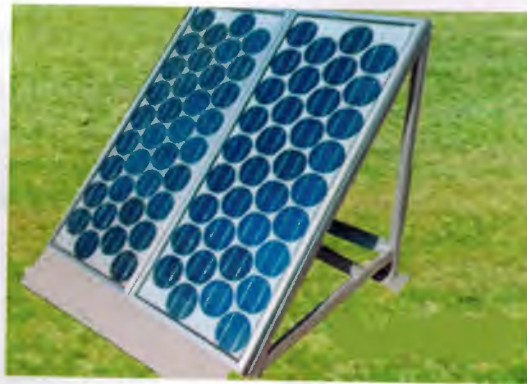


Figure 4.1 PV panels used in experimental work [30].



Figure 4.2 Variable resistance (BOX 1051) [30].



Figure 4.3 Explorer GLX [30].

4.3 Simulation Work

In the current work the simulation process composed of three phases of PV system implementation. Phase one is PV array models and validations, phase two DC/DC converter and MPPT algorithms were implemented and comparison between them were given, and phase three which is DC/AC converter is designed and tested were two controlling strategies are used as shown in the figure 4.4.

Table 4.1 shows the manufacturer's datasheet, by which the data were given under standard test condition (STC), which mean the solar irradiance equal to (1000 W/m^2) and panel temperature equal to (25°C) where K_v and K_i are changing the voltage with temperature, and changing short circuit current with temperature respectively.

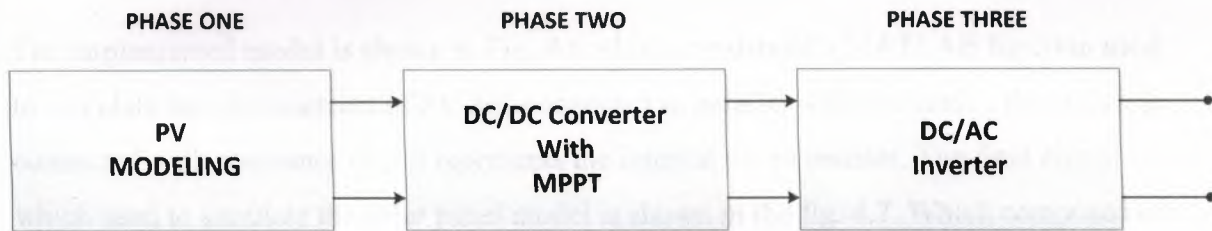


Figure 4.4 Implemented circuit diagram of PV model.

Table 4.1 The manufacture datasheet for NT 111 solar panel.

Parameters	Values
N_s	36
P_m	43 [W]
V_m	17.5 [V]
I_m	2.46 [A]
I_{sc}	2.7 [A]
V_{oc}	21.6 [V]
K_v	-0.0037 [V/K]
K_i	0.0005 [A/K]

4.3.1 Phase One: PV array models

The implementation of the PV models were done by using MATLAB /Simulink package 2012 version, several PV modules are presented in order to find the accurate, simplest, and best performance model which validated by using real time recorded data, the following models are implemented:

4.3.1.1 Model one

The implemented circuits of model one are based on Eqs. 2.7 to 2.14 given in chapter two section 2.12.1. The general circuit of model one given in the Fig. 4.5. The internal circuit of model one which includes the MATLAB function to calculate (I_{ph}) of the array is given in Appendix.

The implemented model is shown in Fig. 4.6 which consists of a MATLAB function used to calculate the photocurrent of PV cell connected in parallel with the diode, the circuit is connected with resistance (R_s) it represents the internal series resistor. The final circuit which used to simulate the solar panel model is shown in the fig. 4.7. Which composed of a PV panel, voltage and current measurements and a load resistor. The simulation results of PV panel are given in the fig. 4.8 and 4.9 which represents the I-V and P-V curve respectively, Table 4.2 shows the simulation result for some unknown parameters of PV panel.

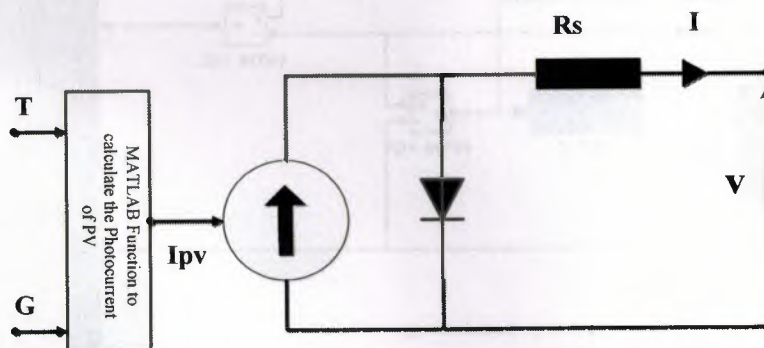


Figure 4.5 Implemented circuit diagram of PV model.

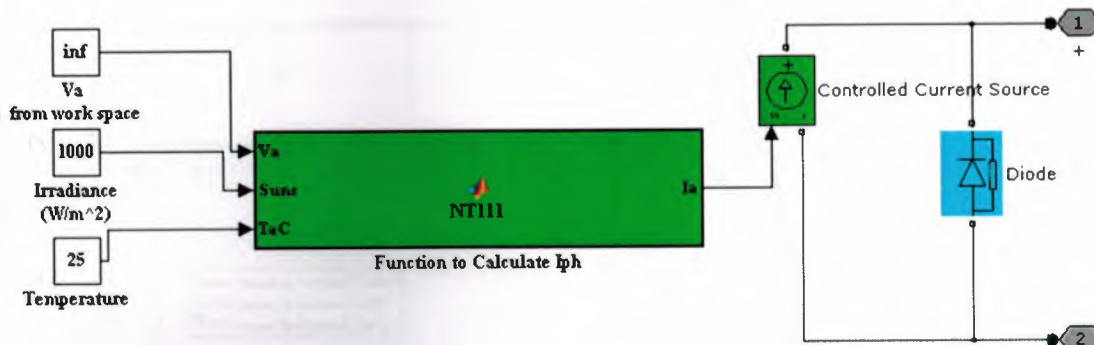


Figure 4.6 The internal circuit diagram of PV array model one.

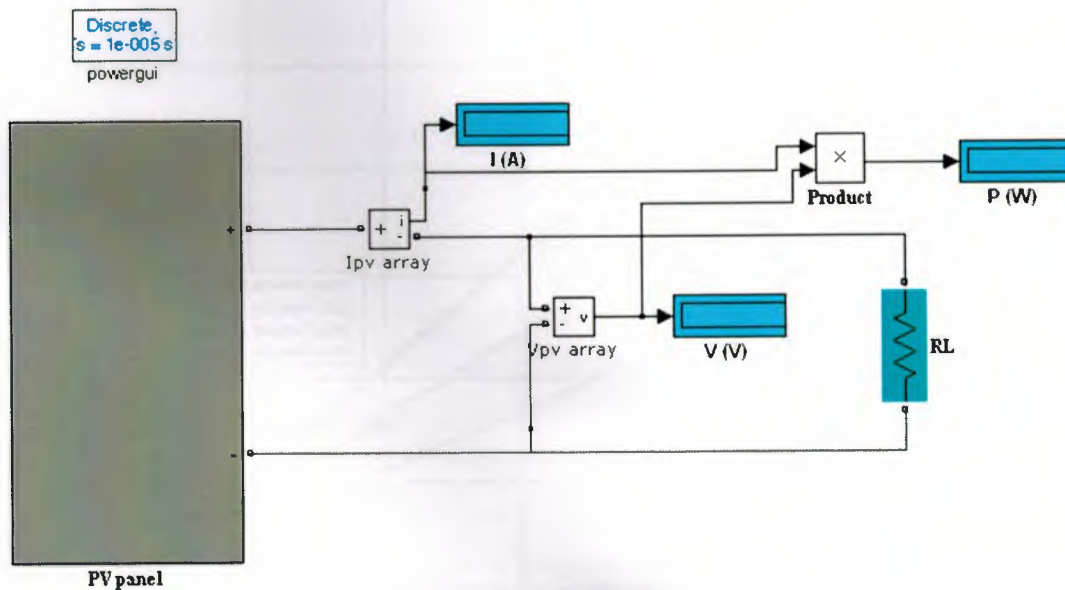


Figure 4.7 The complete circuit diagram of a PV array.

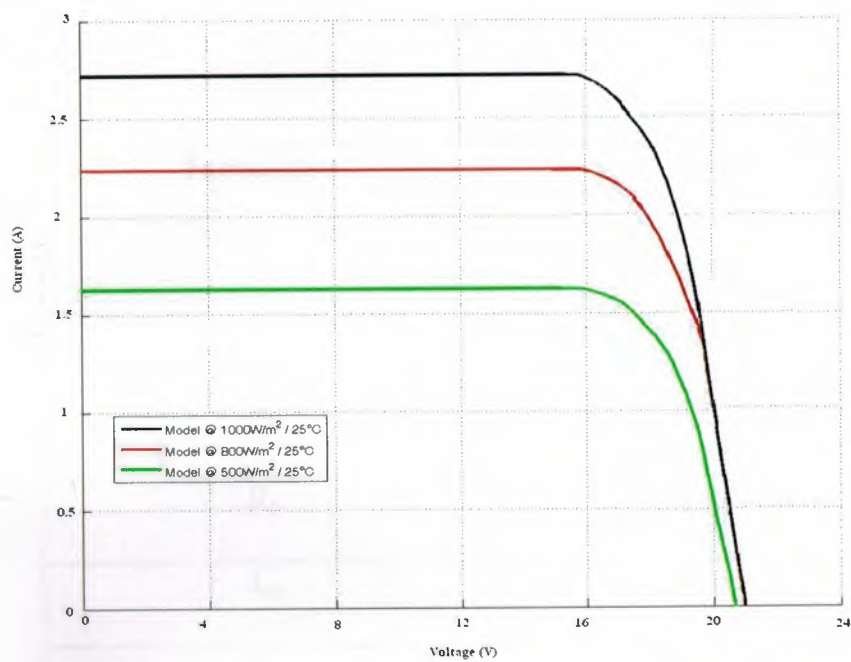


Figure 4.8 The I-V curve of implemented circuit model one.

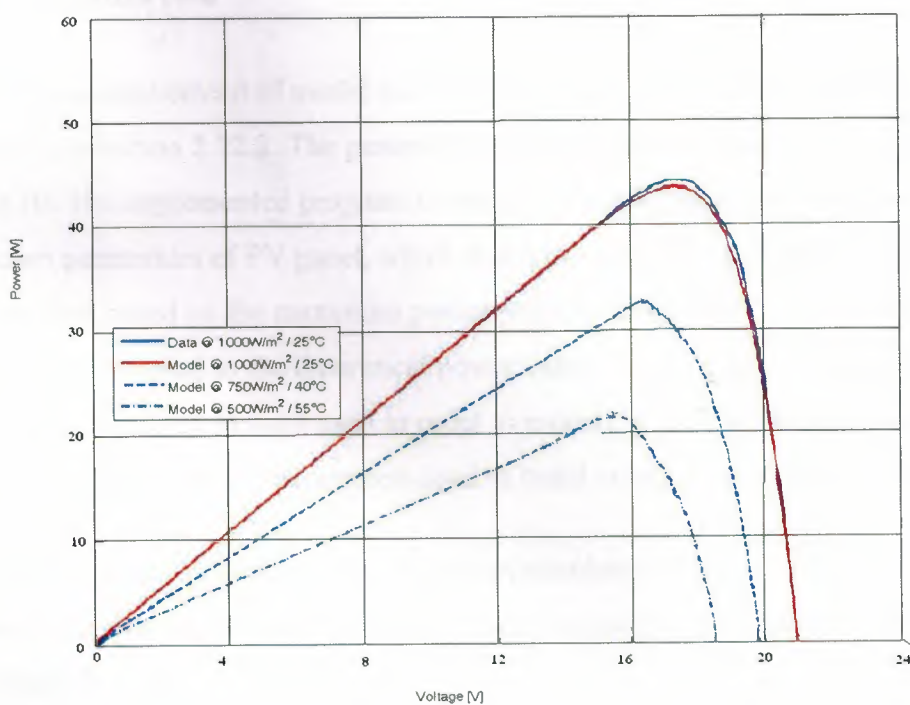


Figure 4.9 The P-V curve of implemented circuit model one.

Table 4.2 Shows the unknown parameters obtained from MATLAB simulation by first model.

Parameters	Values
a	1.2
V_g	1.12 V
R_s	0.162 Ω
R_p	∞ [open circuit]
I_{sa}	9.6e-9 A
I_{ph}	2.69 A

4.3.1.2 Model two

The implemented circuit of model two based on Eqs. 2.15 to 2.23 which are given in chapter two section 2.12.2. The general circuit that represents model two is shown in the Fig. 4.10. The implemented program is using Newton-Raphson method to calculate the unknown parameters of PV panel, which is not provided by the manufacturer datasheet. This method based on the maximum power point; at this point, the value of experimental power of PV is equal to the theoretical power value. In this model mathematical blocks in MATLAB /Simulink in were used in order to modeling the PV panel as shown in the Fig. 4.11, Table 4.3 shows the parameters used to build model two as shown in the Fig. 4.12.

The output results of the implemented circuit simulation shown in the Fig.4.13. (a) and (b) shows the output result of implementing programs and (c) show the experimental test by PV manufactures.

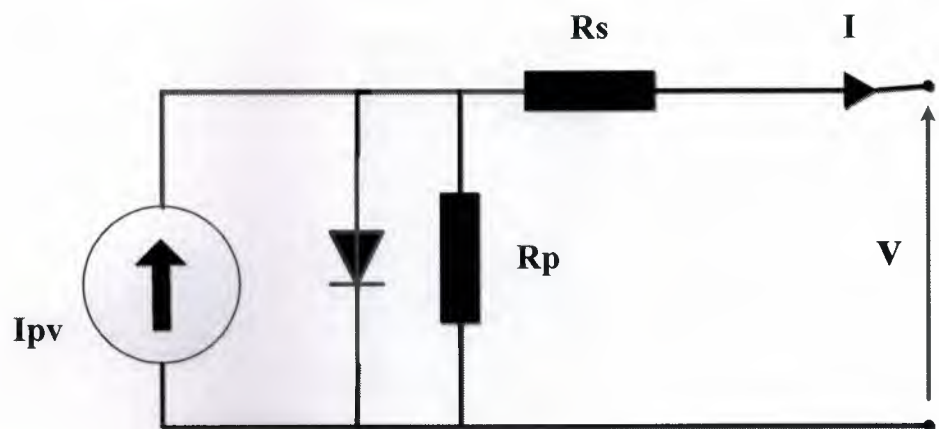


Figure 4.10 The circuit diagram of model two.

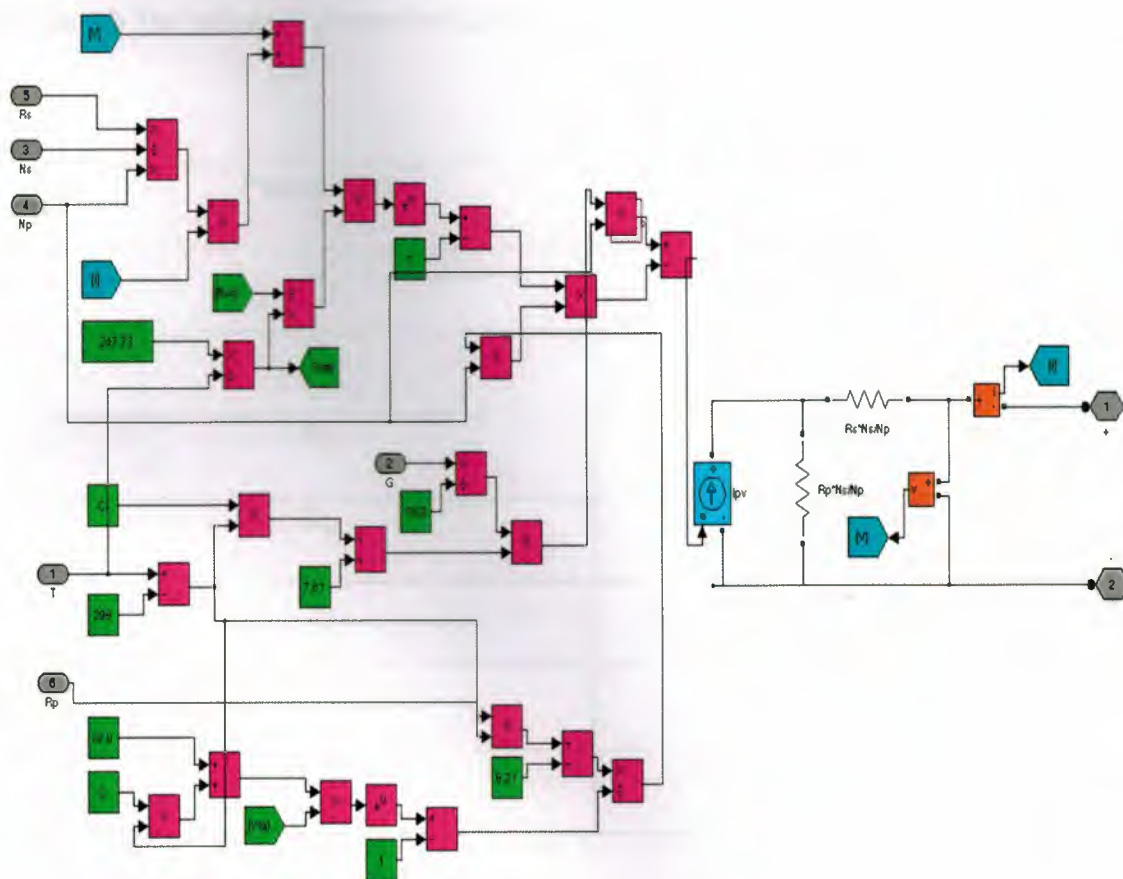


Figure 4.11 The internal circuit diagram of PV array model two.

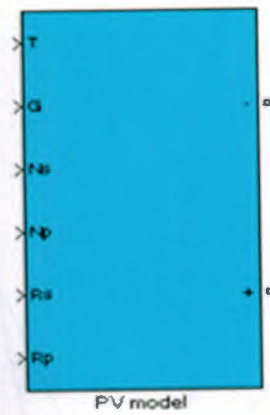


Figure 4.12 The block diagram of PV array model two.

Table 4.3 The unknown parameters obtained from MATLAB simulation by second model.

Parameters	Values
a	1.2
V_g	1.12 V
R_s	580 m Ω
R_p	325.98 K Ω
I_{sa}	9.54143e-009 A
I_{ph}	2.700005 A
$P_{max,m}$	43.170821 W

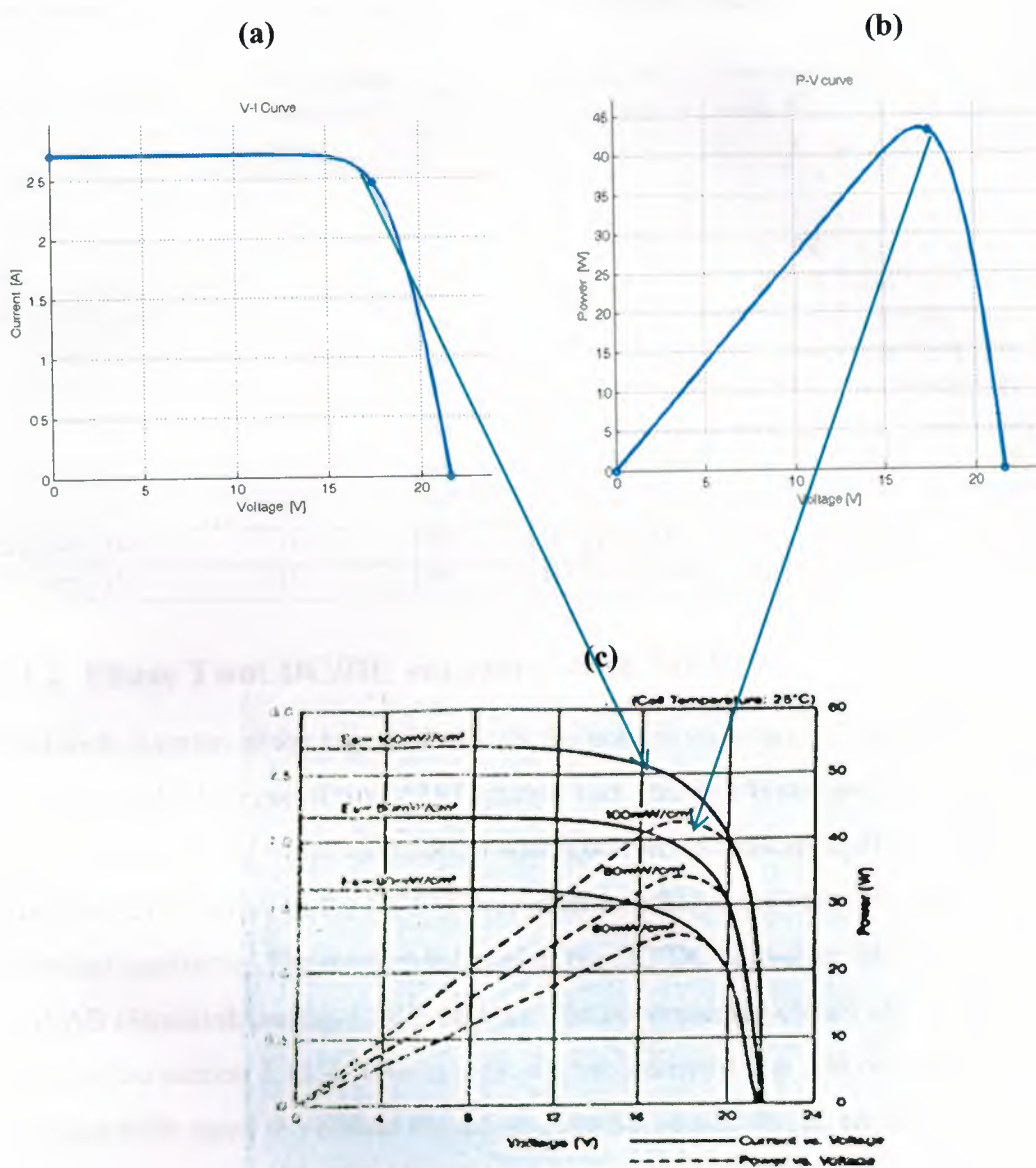


Figure 4.13 Comparison between modeling results and experimental data from data sheet (a) And (b) shows the output results of implemented circuit and (c) show the experimental test by PV manufactures.

From the simulation results in Table 4.4, which were recorded and compared with real data (validation) it is clear that the model one consider the more accurate and simulate the operation of PV panel in real life. Therefore, model one it will be used to implement the solar power generator for domestic load operation.

Table 4.4 The experimental, model one, and model two results.

Months	Ambient Temperature (C)	Back-of-Panel Temperature (C)	Irradiance (W/m ²)	Experimental Result of PV			Simulation Result					
				V	I	P	Model One			Model Two		
							V	I	P	V	I	P
January	13.7	18.1	490	14.2	1.3	18.46	13.35	1.28	17.09	12.23	1.22	14.96
February	15.3	20.1	520	14.5	1.35	19.575	14.12	1.41	19.91	12.99	1.3	16.89
march	18.6	27.4	610	17	1.55	26.35	16.15	1.62	26.16	15.26	1.53	23.35
April	22.6	30.1	710	18	1.65	29.7	17.61	1.76	30.99	17.77	1.78	31.56
may	29.8	37.2	792	18.5	1.6	29.6	17.92	1.79	32.08	19.85	1.98	39.39
June	39	48	826	17.5	1.7	29.75	17.4	1.74	30.28	20.74	2.07	42.93
July	42.5	67	810	15.5	1.55	24.025	16.01	1.6	25.62	20.42	2.04	41.66
August	42	58	736	16	1.59	25.44	16.13	1.61	25.97	18.52	1.85	34.26
September	36.5	45	650	16.5	1.64	27.06	16.01	1.6	25.62	16.31	1.63	26.59
October	28	35.4	565	14.7	1.5	22.05	14.84	1.48	21.96	14.15	1.42	20.09
November	18.5	26.4	510	14	1.2	16.8	14.02	1.29	18.09	11.25	1.13	12.71
December	13.5	17.5	480	13.1	1.4	18.34	13.25	1.3	17.23	9.48	0.95	9.01

4.3.2 Phase Two: DC/DC converter with MPPT

The block diagram of the Fig. 4.14 shows the general structure of DC/DC converter which controlled by use of the MPPT control box, this box is composed from, MPPT algorithm, and Pulse width modulation which converted the duty cycle to pulses used to drive the IGBT device in the DC/DC converter to achieve the maximum power in any operating condition. The implementation of the DC/DC converter was done by using MALAB /Simulink package 2012 version. The implemented circuit of DC/DC converter is based on the section 3.11.2. Two models are implemented, the first one, which composed from one solar panel to validate the design, and the second model composed from multi PV system to achieve the required power for domestic load, according to the ministry of electricity standard (KRG of IRAQ).

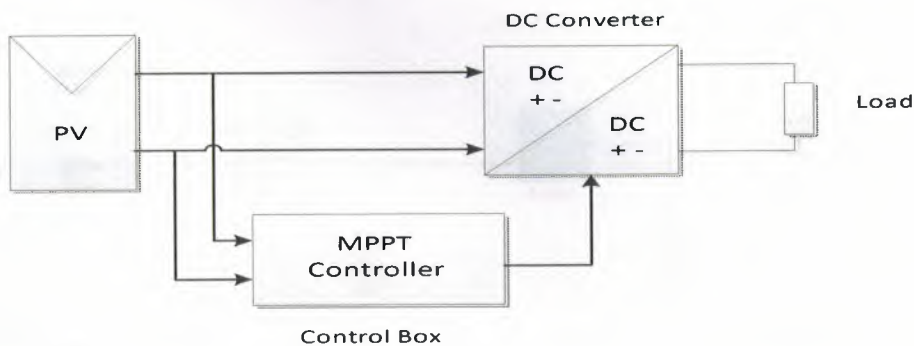


Figure 4.14 The schematic diagram of the photovoltaic simulation system.

The parameters used for modeling a single PV panel is shown in the Table 4.5 these values are calculated according to IEC harmonic standards, these values, are considered as initial values and changed according to experimental results to achieve the best performance and accurate results so, the final values are given in the Table 4.5. Fig. 4.15 shows the buck-boost DC/DC converter which is composed of inductance, capacitance, diode, and IGBT works as a switch.

Table 4.5 The calculated parameters values of DC/DC converter.

V _{in}	13- 17 V
V _{out}	20- 24 V
L _{min}	37.5 μH
C _{min}	1670 μF
Duty Cycle	Boost mode => 0.5 and Buck mode <= 0.5
Switching frequency	100 kHz
R _{load}	30 Ω

Table 4.6 L-C Experimental values of DC/DC converter.

L	90 μH
C	2000 μF

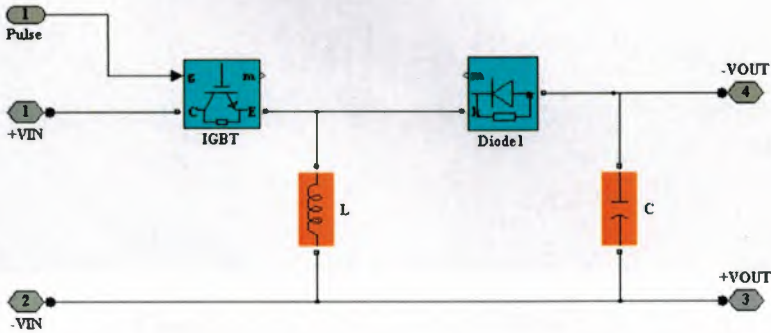


Figure 4.15 The circuit diagram of buck boost converter.

In order to verify and compare the effects of the MPPT algorithms for the photovoltaic simulation system, some test cases implemented under different irradiance, temperature and load conditions to observe whether the output power of the photovoltaic system can reach the maximum power of the solar modules. Table 4.6 shows the sample of testing parameters. The simulated results are given in the Fig. 4.16 to 4.19. These figures are show the change in the load resistor, irradiance, and temperature.

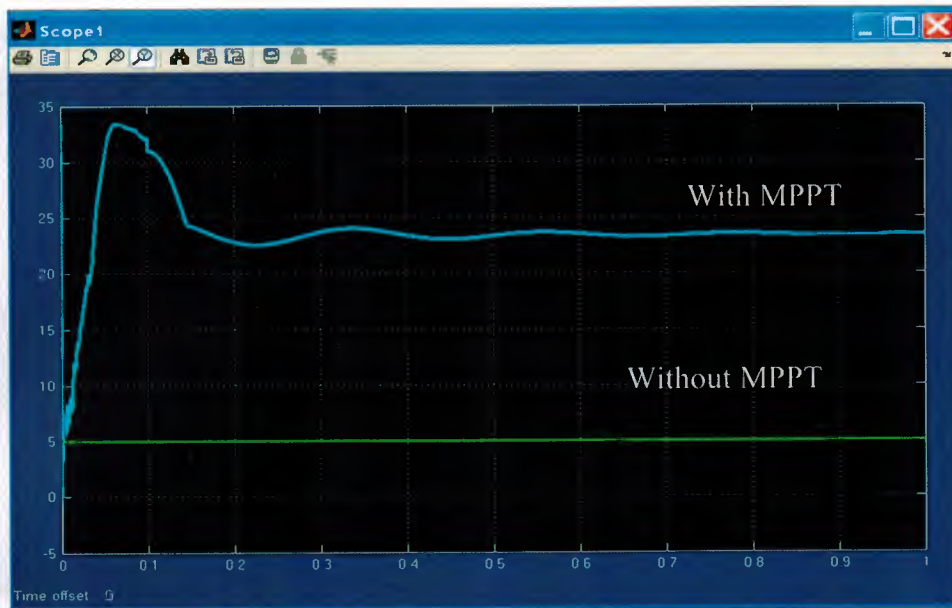
Table 4.7 Shows the test data for implemented MPPT system.

Cases	Load Resistor (Ω)	PV power Without MPP (W)	PV power With MPP (W)	Irradiance (W/m^2)	Temperature ($^{\circ}\text{C}$)
Case 1	50	9.25	41.5	1000	25
Case 2	85	5.6	30.4	800	25
Case 3	20	21	42	1000	25
Case 4	30	14.48	29	800	25



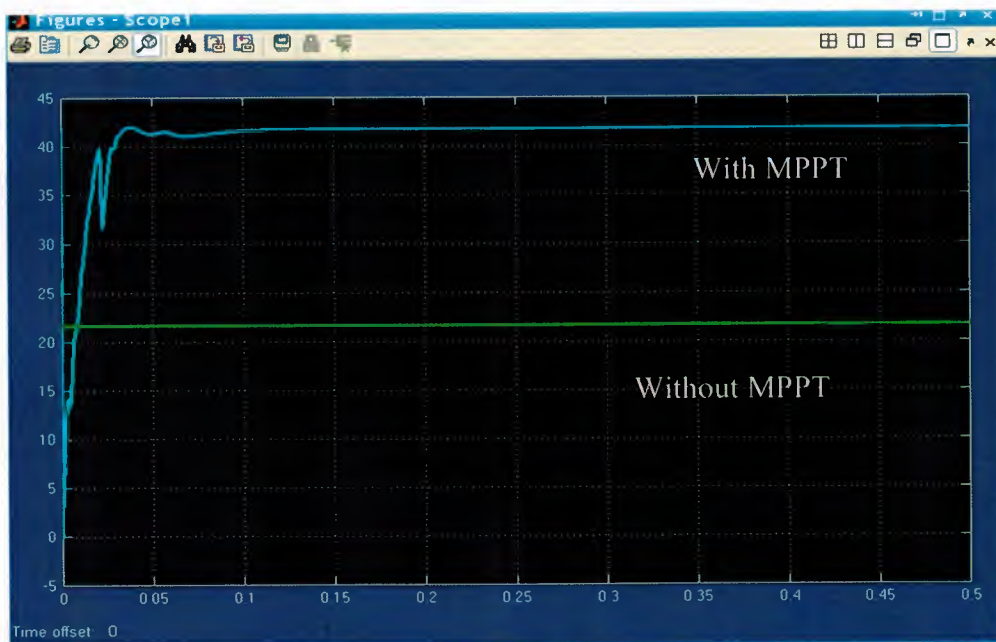
Case 1: $R=50(\Omega)$, $I_r=1000$ (W/m^2), $T= 25$ (C).

Figure 16 Simulation Result of case 1.



Case 2: $R=85\ (\Omega)$, $I_r=800\ (W/m^2)$, $T=25\ (C)$.

Figure 17 Simulation Result of case 2.



Case 3: $R=20(\Omega)$, $I_r=1000\ (W/M^2)$, $T=25\ (C)$.

Figure 18 Simulation Result of case 3.



Case 4: $R=30(\Omega)$, $I_r=800$ (W/M²), $T= 25$ (C).

Figure 19 Simulation Result of case 4.

4.3.3 Phase Three: DC/AC inverter

The implemented circuit of DC/AC converter shown in the Fig. 4.20. This circuit is powered by 220 V DC and full bridge IGBT connected to supply a load with a capacity of 1KW, and 220V AC , these load parameters simulate the required power which provides a domestic load. The control of VSI is based on the PI controller were used to control voltage and current. The output result of the DC/AC inverter is shown in the Figure 4.21.

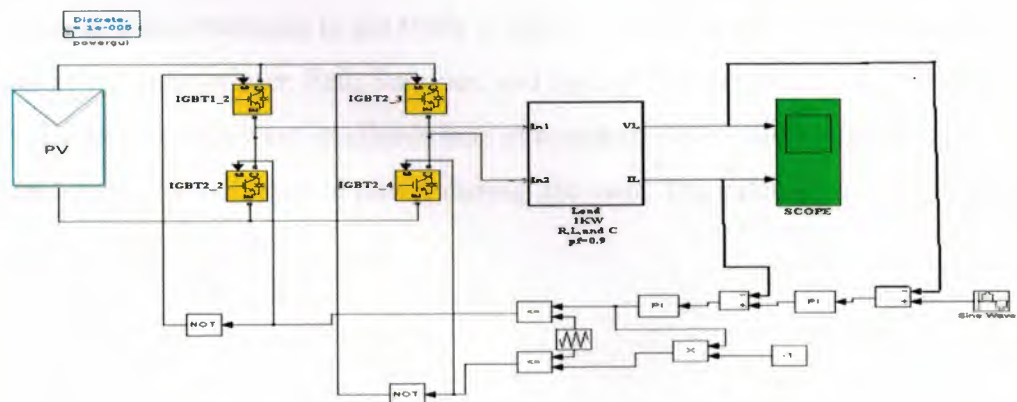


Figure 4.20 Implemented circuit of DC/AC converter.

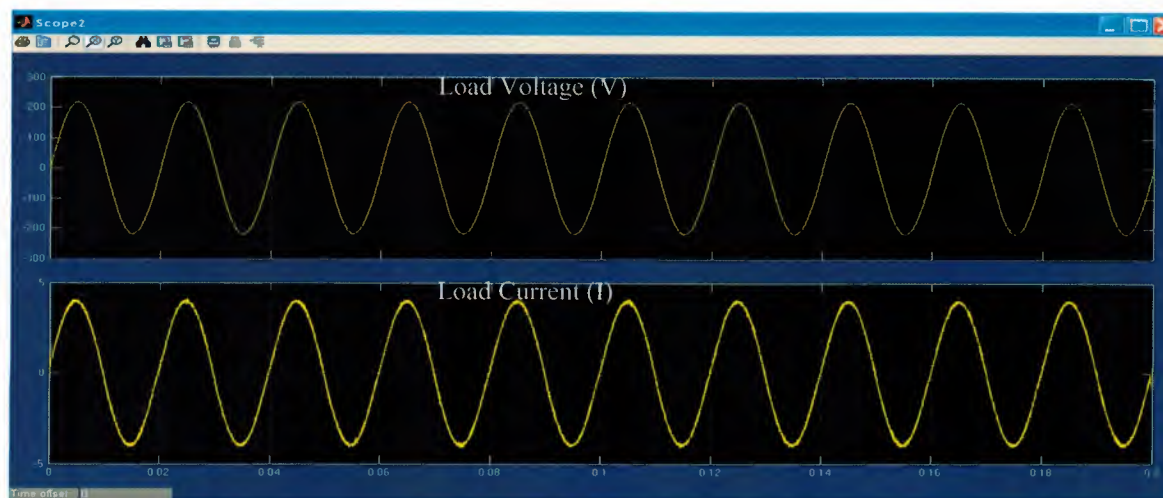


Figure 4.21 Simulation results waveforms of the load voltage and current.

4.4 Solar Power Generator Design for Domestic Load

The ultimate objective of this thesis is to design an economic and environmentally friendly source of energy for domestic load according to [30] the 99% of households in (Koya city/ KRG of IRAQ) consumed a current equal or less than to (4A) for 6 hours per day, supplied by private generators in the city.

The parameters were used to design the solar power generator system under IEC harmonic standard and ministry of electricity. Where the PV panels used in design is NT 111 Sharp Co. Product with maximum power equal to (43W) under STC, the solar model for panel module used is model one. According to this model recorded result very close to real data.

The existing solar irradiance in the study is divided into four part which represent the year seasons of the year (winter, Fall, Summer, and Spring) as shown in the Table 4.9, the selected season with lowest irradiance was in winter to ensure the designed solar power generator provides the required power during the year. The calculation used to design the solar power generators are.

– PV sizing:

P_{PV} The irradiance in winter session (W)

$$P_{PV} = 18.7 \text{ (W)}$$

$$E_{PV} = 18.07 * t_d = 18.07 * 10 = 180.7 \text{ Wh/day}$$

Where t_d Is daylight in hour / day;

Table 4.8 shows the different solar parameters such as t_d , Current, voltage, power, and energy recorded in the study area.

$$E_{PV} = \frac{180.7}{PV \text{ area}} = \frac{180.7}{0.504} = 359 \text{ Wh/m}^2/\text{day}$$

This value is existing solar energy in the winter session.

The required power is 1 kw with PF=0.9

$$P = V * I * \cos \alpha = 220 * 4 * 0.9 = 792W$$

The power used by PV system supply the householder for six hours per day at daylight period when the grid utility always supply electricity at night.

$$E_{req} = P * t_0 = 792 * 6 = 4752 \text{ Wh/day}$$

Where t_0 is equal to operation time of load =6 hours/day

Assume that the efficiency of DC/DC converter and DC/AC converter be equal to 0.8.

$$\eta = \frac{E_0}{E_i}$$

$$0.8 = \frac{E_{req}}{E_i}$$

$$E_i = \frac{E_{req}}{0.8} = \frac{4752}{0.8} = 5940 \text{ Wh/m}^2/\text{day}$$

$$\text{The required area of PV panels} = \frac{\text{Required Energy}}{\text{Existing Energy}} = \frac{5940}{359} = 16.5 \text{ m}^2$$

$$\text{Number of PV panels required} = \frac{\text{Area of PV Required}}{\text{Area of one PV panel}} = \frac{16.5}{0.504} = 32.8$$

The minimum number of PV is equal to = 33

In the current design, the number of PV panels used is 35 PV's

The connection is five PV's in parallel to supply current equal to 8 A minimum values as shown the fig.4.22.

And 6 groups of above group connected to supply 140 V minimum values (series connection) shown in Fig 4.23, the overall system connected directly to the DC/AC inverter as shown in the Fig. 4.24.

- DC/DC converter sizing

The DC/DC converter connected in string topology so, each panel connected directly with DC/DC converter individually the values of parameters used are shown in Table 4.10.

- DC/AC inverter sizing

The net power required to supply the load by inverter is 1000 W. According to IEC standard and for safety operation the inverter should be considered 25-30% bigger than the power required.

Therefore:

$$p_{inv} = p_{req} + p_{req} * 0.3 = 1000 + 300 = 1300 \text{ W}$$

The total circuit is shown in the fig. 4.25 and the output result is given in the fig.4.26

Table 4.8 The day length and clearness index.

Months	Day length (h/day) t_d	Clearness Index K_t
January	9.98	0.7
February	10.86	0.77
march	11.97	0.78
April	13.05	0.76
may	14.09	0.72
June	14.58	0.69
July	14.41	0.66
August	13.5	0.66
September	12.45	0.67
October	11.4	0.67
November	10.28	0.7
December	9.75	0.74

Table 4.9 Average seasons solar irradiance, in studied area.

Seasons	Voltage V (V)	Current I (I)	Power P (W)	Energy (W/m ²) E	Daylight length (h/day) t_d	Energy (Wh/m ² /day) E_t
Winter	13.6	1.33	18.08	35.78	10.1	361.3
Spring	17.3	1.6	27.68	54.92	13.3	730.4
Summer	16.5	1.65	27.2	54	14.1	761.4
Fall	14.9	1.45	21.6	42.85	11.37	487.2

Table 4.10 Shows the parameters used to configure the DC/DC converter.

V_{in} (average value)	140 V
V_{out} (Average Value)	400 V
L	47 μ H
C	2000 μ F

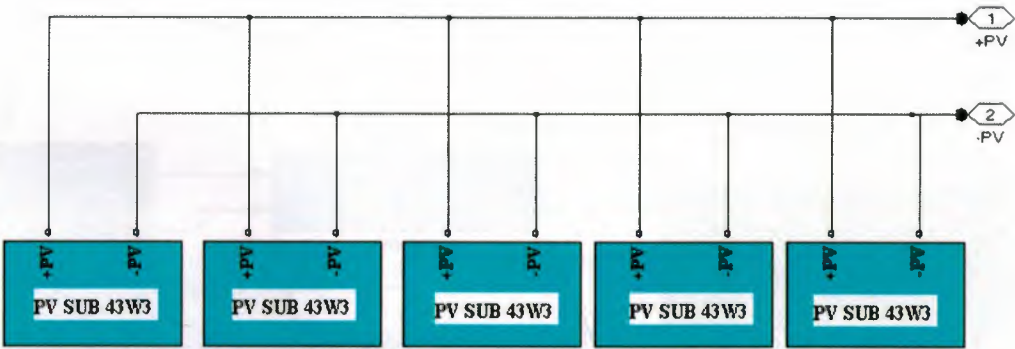


Figure 4.22 Parallel connection of PV panels.

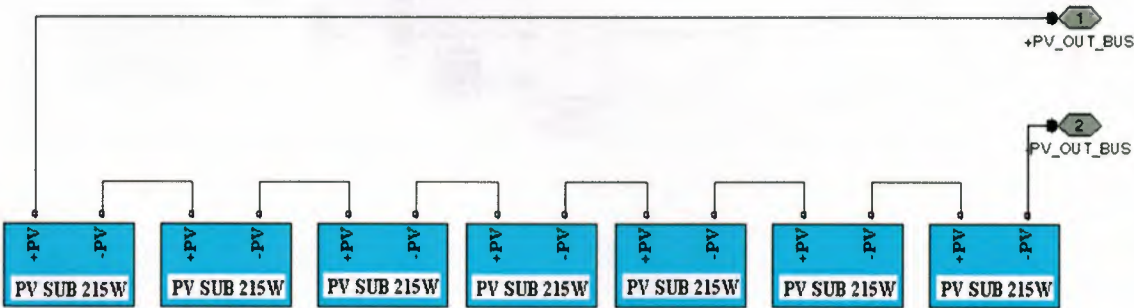


Figure 4.23 Series connection of PV panels.

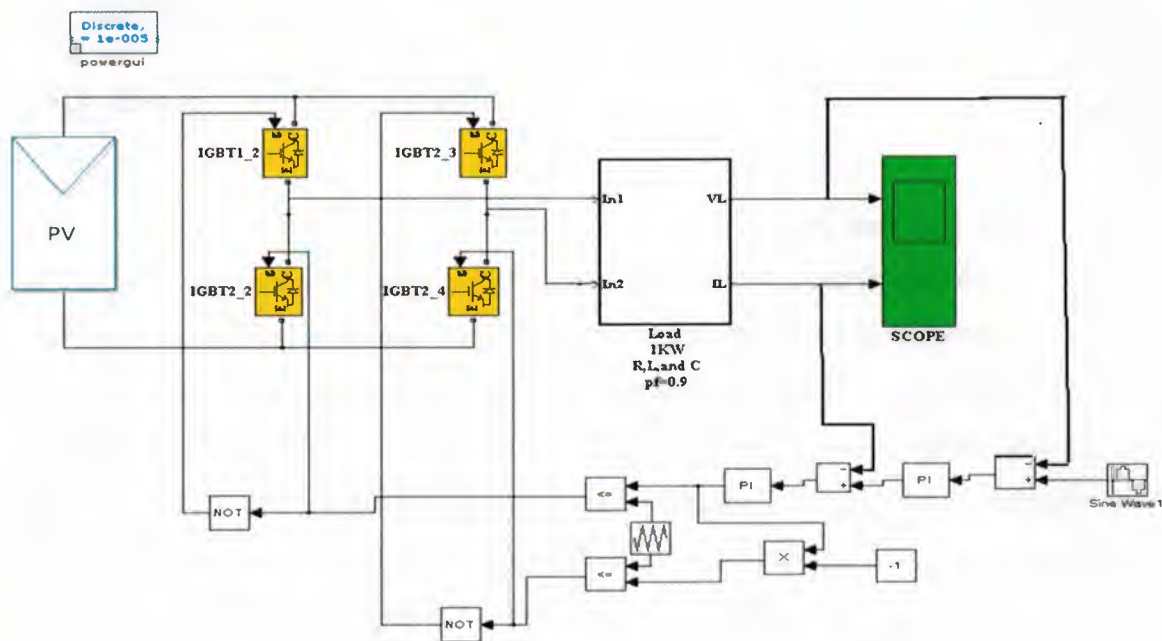


Figure 4.25 Inverter connected with PV panel.

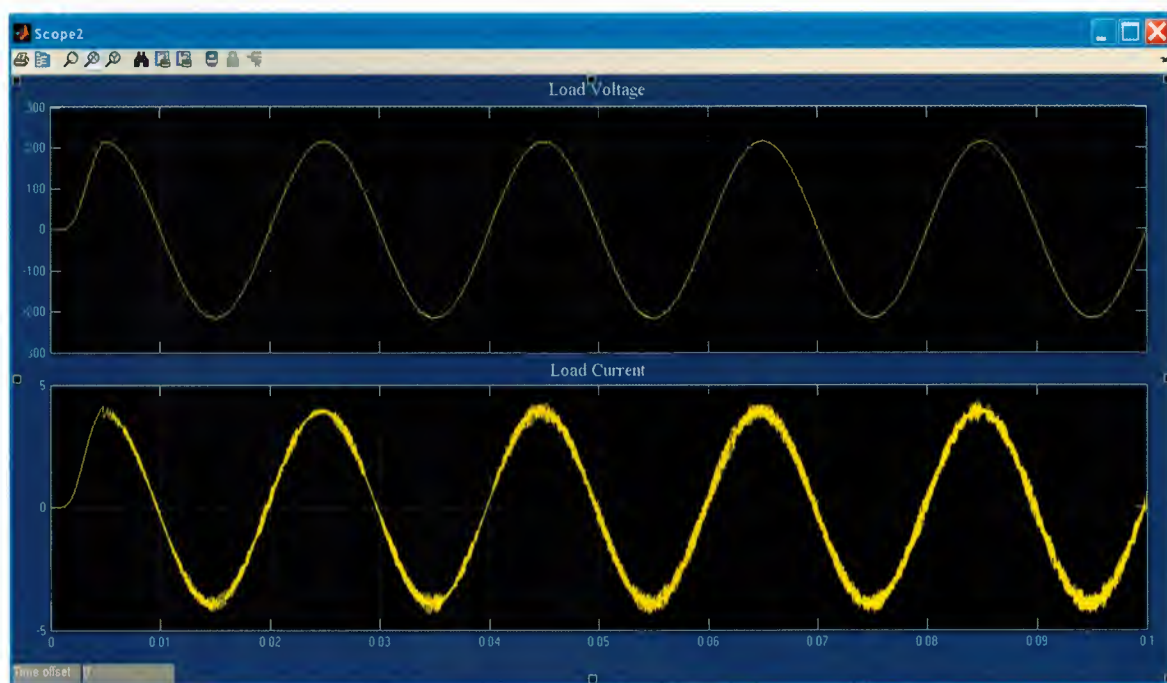


Figure 4.26 Simulation waveform of implemented system for domestic load.

4.5 Results Discussion

4.5.1 Phase One: PV modeling

In phase one two PV panels of the PV modeling system were designed and simulated to find the best one used to supply DC/DC converter. Table 4.3 and figures 4.8, 4.9, and 4.13, show the output results of model one and model two of PV panels respectively. From the simulation, results it's clear that the two models simulate the real operation of PV panels under STC, but for real life application model one has better accuracy and operation behavior according to simulation results which compared with validation data. For model one simulation, all unknown parameters are calculated directly therefore, it takes a long time in the simulation process, but for model two the unknown parameters are calculated offline, by the help of an individual program, after that the output results are used to configure the parameters of fig. 4.11. All above results implemented by the use of back of panel temperature, which is different from the ambient temperature as shown in Table A1 in appendices.

4.5.2 Phase Two: DC/DC converter with MPPT controller

The DC/DC converter implemented in this thesis presented in the FIG. 4.15 it's a simple buck-boost converter, the parameters of the converter are selected according to IEC standard for harmonic and required operation.

Figs. 4.16 to 4.19 shows the operation of implemented DC/DC converter from the implemented results it's clear that the operation of DC/DC converter always gives the maximum power of PV under variation in the load and weather conditions. The P&O algorithm was used to control a DC/DC converter it succeeded to track the maximum point according to the simulation results.

4.5.3 Phase Three: DC/AC inverter

The simulation results of the implemented inverter are shown in the Figs. 4.21 and 4.26, these two figures represented the load voltage and current, from these two waveforms it's clear that the output of inverter in sinusoidal waveform and includes a harmonic due to the non-linear load connected with the inverter.

Fig. 4.26 shows the output of the overall PV system. This system used to supply a domestic load in the study area, from this figure it's clear that there are distortion in the current and voltage waveforms especially at time (0.005 s) at this time the distortion is very clear, this distortion is due to the delay in the PV processing where a (35) panel used to supply 1KW, also the changing in the output of DC/DC converter. The control approach used was PI controller, in this type of controllers two parameters Proportional gain (K_p), and Integral gain (K_i) were changed many times in order to achieve better results.

CHAPTER FIVE

CONCLUSIONS

A novel approach to solar power generator was developed. The novelty of this work is using real life data, which was recorded under different weather conditions, also a new approach to measure the solar cell parameters by the use of back panel temperature as a modeling temperature. In this thesis a complete model of solar power generator is presented composed of, two solar cells, MPPT controller, DC/DC buck-boost converter, and inverter where all of them were implemented and tested with validation data.

The implemented system is divided into three phases, where each phase is implemented and simulated also the results are given and discussed. Phase one was implemented by two solar cell models, a comparative study of two models show that model one has better accuracy and operation behavior according to simulation results which were compared with validation data.

Phase two was MPPT algorithm, where a P&O algorithm was used, the simulation results show that the presented algorithm gives an efficiency close to steady state operation. The MPPT controller used to control a buck boost converter. From the simulation result of DC/DC converter it's clear that, the implemented circuit of DC/DC converter with MPPT algorithm succeed to track the maximum power operation of PV panel under change the load and weather conditions. The designed DC/DC converter depended mainly on the ripple factor of voltage and current required, also on the duty cycle of DC/DC converter.

Phase three an inverter circuit to convert the DC input to AC was implemented and tested. The control approach used was PI controller, from the simulation results it is clear that the output of the inverter is close to a sine wave signal which is required.

The proposed system to supply domestic load was implemented and the simulation results were presented, from simulation results it's clear that the output of DC/AC inverter could be used directly to supply load composed of L, C, and R with PF equal to 0.9.

A real life application has been addressed in this work; the proposed model could be successfully used to supply the householders according to validation data (real life data) and simulation results.

FUTURE WORK

The simulation results achieved in this thesis could be considered as a driven force for future work, for instance to build a prototype model to test the implemented solar power generators in the Laboratory. The model should be developed to include some important stages such as: charger control and battery, grid connected system, and a very promised aspect is the use of PV panels with DC bus bar for a domestic load.

REFERENCES

- [1] Kosarian, A., and Jelodarian P. (2011). Efficiency Improvement by Optimization of Absorber Layer and n-Layer in a-Si:H/a-SiGe:H Advanced Thin Film Solar Cells. IEEE Journals Computational Intelligence, Modeling and Simulation 978: 7695-4562.
- [2] Ashraf, I. (2006). Estimation of CO₂ Mitigation Potential through Renewable Energy Generation. 2006 IEEE International Power and Energy Conference, (i), 24–29.
- [3] Persall, N., and Hill, R. (2001). Photovoltaic Module, systems and application. (2nd ed.) North Umbria, University of North Umbria at Newcastle.
- [4] Kachhiya, K., Lokhande, M., and Patel, M. (2011). MATLAB/Simulink Model of Solar PV Module and MPPT Algorithm. National Conference on Recent Trends in Engineering and Technology. B.V.M. Engineering College, V.V.Nagar, Gujarat, India.
- [5] Kothari, D. (2000). Renewable Energy Scenario in India. IEEE Journals, 6: 643-636.
- [6] Hamakawa, Y. (2004). Thin-Film Solar Cells: Next Generation Photovoltaic and Its Applications. (Ed.) Springer-Verlag , Germany.
- [7] Mohammed. SH. (2009). Street and House Lighting Using PV Panel, a thesis submitted to the council of College of Engineering University of Salahaddin.
- [8] Shah, A. (2010). Thin-Film Silicon Solar Cells. (1st Ed.) CRC Press, Taylor and Francis Group, LLC, Retrieved Jan 10, 2013, from <http://books.google.com.cy/books?id=DBSkX6w0rFMC&printsec=frontcover&hl=ar#v=onepage&q&f=false>.
- [9] Yung Lo, S., Wu S., Chang, C., Wang. C., Lien S., and Horng R. (2011). Fabrication of Flexible Amorphous-Si Thin-Film Solar Cells on a Parylene Template Using a Direct Separation Process. IEEE Transaction on Electronic Devices, 58: 51.
- [10] Aliyu, M., Hamzah R., Islam A., Matin, M., Karim, R., Sopian, K., and Amin N. (2012). The Significance of Substrate Surfaces in Flexible Thin Film CdTe Solar Cells Fabrication. Developments in Renewable Energy Technology (ICDRET), 2nd IEEE International Conference. 1- 4.

- [11] ALQahtani H., A., Abuhamdeh S., M., and Alsmadi M., Y. (2012). A Simplified and Comprehensive Approach to Characterize Photovoltaic System Performance. Energytech, IEEE. Ohio State Univ., Columbus, OH, USA, 1-6.
- [12] Subudhi, B., and Pradhan, R. (2012). A Comparative Study on Maximum Power Point Tracking Techniques for Photovoltaic Power Systems. *IEEE Transaction on Sustainable Energy*. 4(1), 89-98.
- [13] Eshram, T., and Chapman P., L., (2007). Comparison of photovoltaic array maximum power point tracking techniques, *IEEE Trans. Energy Conv.*, 2(22), 439–449.
- [14] Khatib T., Mohamed, A., Amin, N., and Sopian, K. (2010). An efficient maximum power point tracking controller for photovoltaic systems using new boost converter design and improved control algorithm. *WSEAS Trans. Power System*, 2(5), 53–63.
- [15] Phang, J., Chan D., and Phillips J. (1984). Accurate analytical method for the extraction of solar cell. *Electron. Letters*, 10(20), 406–408.
- [16] Carrero, C., Amador, J. and Arnaltes, S. (2007). A single procedure for helping PV designers to select silicon PV module and evaluate the loss resistances. *Renewable Energy*, 32(15), 2579–2589.
- [17] Ngan, M., Tan, C. (2011). A Study of Maximum Power Point Tracking Algorithms for Stand-alone Photovoltaic Systems. *IEEE Power Electronic Colloquium*, 22-27.
- [18] Salas, V., Barrado, A., Lazaro, A. (2006). Review of the Maximum Power Point Tracking Algorithms for Stand-alone Photovoltaic Systems, *Solar Energy Materials and Solar Cells*, 1555–1578.
- [19] Salmi, T., Bouzguenda M., Gastli, A., and Masmoudi, A. (2012). MATLAB/Simulink Based Modeling of Solar Photovoltaic Cell. *International Journal of Renewable Energy Research*, 2 (2).
- [20] Bellini, A., Bifaretti, S., Iacovone, V., Cornaro, C. (2009). Simplified Model of a Photovoltaic Module. Dept. of Electronic Engineering, University of Rome Tor Vergata.
- [21] Walker, G., (2001). Evaluating MPPT converter topologies using a MATLAB PV model. *J. Elect. Electron. Eng. Australia*, (21), 49 -56
- [22] ČORBA, Z., KATIĆ, V., DUMNIĆ, B., and MILIĆEVIĆ, D. (2012) In-Grid Solar-To-Electrical Energy Conversion System. *Modeling and Testing. Thermal Science*, (16), S159-S171

- [23] Barchowsky, A., Parvin, Jeffrey P., Reed, Gregory F., Korytowski, Matthew J., Grainger, Brandon M.(2012). A Comparative Study of MPPT Methods for Distributed Photovoltaic Generation. *Innovative Smart Grid Technologies*. 1-7.
- [24] Suwannatrai P., Liutanakul, p., and Wipasuramonton, P. (2011). Maximum Power Point Tracking by Incremental Conductance Method for Photovoltaic Systems with Phase Shifted Full-Bridge dc-dc Converter. *Electrical Power Systems Energy Conversion*, 637-640.
- [25] Femia, N., Member, Petrone, G., Spagnuolo, G., and Vitelli, M. (2005). Optimization of Perturb and Observe Maximum Power Point Tracking Method. *IEEE Transactions on Power Electronics*, 4 (20), 963-973.
- [26] De Brito, Moacyr Aurelian, Galotto, Luigi; Sampaio, Leonardo Poltronieri, de Azevedo e Melo, G.,Canesin, Canesin Alberto.(2013). Evaluation of the Main MPPT Techniques or Photovoltaic Applications. *IEEE Transactions on Industrial Electronics*, 3 (60), 1156-1167.
- [27] Ting-Chung, Y., Yu-Cheng, L. (2011). Establishment and Study of a Photovoltaic System with the MPPT Function. Longhua Science and Technology University.73-84.
- [28] Persall, N., and Hill, R. (2001). Photovoltaic Module, systems and application. (2nd ed.) Northumbria , University of Northumbria at Newcastle.
- [29] Renewable Energy (2009). *Microsoft Student 2009 DVD*. Redmond, WA: Microsoft Corporation. *In text*: ("Renewable Energy," 2009).
- [30] Abbas, H., Alkalefa, Sh. (2011). Spatial Planning of Solar Energy Resource by Using GIS. A Diploma Thesis Faculty of Engineering Duhok university, Iraq.
- [31] Timbus, A., Liserre, M., Teodorescu, R., Rodriguez, P., and Blaabjerg, F., (2009) . Evaluation of Current Controllers for Distributed Power Generation Systems. *IEEE Transaction of Power Electronic*, 3(24), 654-664.
- [32] Femia, N., Petrone, G., Spagnuolo, G., and Vitelli, M. (2005). Optimization of perturb and observe maximum power point tracking method. *IEEE Transaction of Power Electronics*, 4 (20), 963-973.
- [33] Armaroli, N., Balzani, V. (2006). The Future of Energy Supply: Challenges and Opportunities. *Angewandte Chemie International Edition*, 2(46), 52-66.
- [34] International Energy Agency, Solar Energy *Executive Summary*, Retrieved March10, 2013, from <http://www.iea.org/Textbase/npsun/solar2011SUM.pdf>.

- [35] Kalogirou, S. (2009). *Solar Engineering Processes and Systems*. (1st ed.). Academic Press. London, UK.
- [36] Fayaz, M. (2009). Planning for Solar Energy as an Energy Option for Palestine. *Al-Najaah Journal of urban and regional planning/Al-Najaah university*, 15 ,54-56
- [37] Gordon, M. (2001). *Solar Energy the State of the Art*. (1st ed.). James and James Ltd. William Road London, UK.
- [38] Casal, F., Kesselring, P., Winter C. (1987). *Solar Thermal Power Plants Achievements and Lessons Learned Exemplified by the Sps Project in Almeria/Spain*. Springer. New York, NY 10036, USA.
- [39] Gevorkian, P., (2008). *Solar Power in Building Design*. McGraw Hill Professional, NY, USA.
- [40] National Renewable Energy Laboratory (2012). Solar Photovoltaic Technology Basics. Retrieved Jan 10, 2013, from http://www.nrel.gov/learning/re_photovoltaics.html.
- [41] Tiwari, G., Dubey, S. (2010). *Fundamentals of Photovoltaic Modules and Their Application*. Published by royal society of Chemistry, Cambridge, UK.
- [42] Poortmans, J., Arkhipov, V. (2006). *Thin Film Solar Cells: Fabrication, Characterization and Applications*, John Wiley and sons Ltd. West Sussex, UK.
- [43] Yung Lo, S., Wu S., Chang, C., Wang. C., Lien S., and Horng R. (2011). Fabrication of Flexible Amorphous-Si Thin-Film Solar Cells on a Parylene Template Using a Direct Separation Process. *IEEE TRANSACTIONS ON ELECTRON DEVICES*, 58: 51.
- [44] Otto, T. (2009). *Comparative Study of Grid Connected Photovoltaic Arrays*. A MSC Thesis Faculty of San Diego State University.
- [45] Tiwari, G., Dubey, S. (2010). *Fundamentals of Photovoltaic Modules and Their Application*. Published by royal society of Chemistry, Cambridge, UK.
- [46] Villalva, G., Gazoli, R. and Filho, R. (2009). Modeling and circuit-based simulation of photovoltaic arrays,” *Power Electronics Conference, IEEE, Brazilian*, , 1244 - 1254.
- [47] Francisco M., González, L.(2005). Model of Photovoltaic Module in Matlab. Do Congreso Iberoamericano de Estudiantes de Ingenieria Electrical and Electronic, 1-5.
- [48] Yazdani, A., Iravani, R. (2010). *Voltage-sourced converters in power systems: modeling, control, and applications*. John Wiley and Sons, Ltd., US.

- [49] Gordon, M. (2001). Solar Energy the State of the Art. (1st ed.). James and James Ltd. William Road London, UK.
- [50] Rakotomananandro, R. (2012). Study of Photovoltaic System. A MSc Thesis Graduate School of The Ohio State University, USA.
- [51] Jackson, F., Dragon, G. (2008). Planning and installing photovoltaic systems : a guide for installers, architects, and engineers.(2ed). Typeset by Mapset Ltd, Gateshead, UK.
- [52] Yazdani, A., Iravani, R. (2010). Voltage-sourced converters in power systems: modeling, control, and applications. John Wiley and Sons, Ltd., US.
- [53] Rashid, M., (2001). Power Electronic HandBook. Academic Press, San Diego, USA.
- [54] Harjai, A., Bhardwaj, A., and Sandhibigraha, A. (2010). Study of Maximum Power Point (MPPT) in Solar Photovoltaic array. A BSc Projects Department of Electrical Engineering National Institute of Technology, India.
- [55] DAS, D., PRADHAN, S. (2011). Modeling and Simulation of PV Array With Boost Converter: An Open Loop Study. A BSc Projects Department of Electrical Engineering National Institute of Technology, India.
- [56] Vodovozov, V. (2010). Introduction to Power Electronics. Ventus Publishing APS, USA.
- [57] Kharagpur .(2010). Power Electronic . John Wile and sons Ltd. West Sussex, UK.
- [58] MÄKI, A, (2010). Topology of a silicon-based grid-connected photovoltaic generator. A MSc thesis Faculty of Computing and Electrical Engineering Tampere university of Technology.
- [59] Priyadarshane, L. (2010). Modeling and Control of Hybrid AC/DC Micro Grid. A MSC Thesis Department of Electrical Engineering National Institute of Technology, India.
- [60] Schimpf, F., Norum, L. (2008). NORPIE/2008, Nordic Workshop on Power and Industrial Electronics.
- [61] Akihiro Oi. (2005). Design and Simulation of Photovoltaic Water Pumping System. A MSC Thesis Faculty of California Polytechnic State University, San Luis Obispo. USA
- [62] Kharagpur .(2010). Power Electronic converter . John Wile and sons Ltd. West Sussex, UK.

- [63] Nisir, B.(2004). Power Electronics and Their Application in Power System. (1ed). Hawijah Technical Institute Press, Iraq.
- [64] Čorba, Z., Katic, V., Duminc, A., and Milicevic, D.(2012). In-Grid Solar -To-Electrical Energy Conversion System Modeling and Testing. THERMAL SCIENCE, 1(16), S159-S171.
- [65] Buck-Boost Converter . (2009). In http://en.wik/wiki/Buckboost_converter.Retrieved January 20, 2013, from <http://www.wikipedia.com>.
- [66] Salam, Z. (2003). Power Electronics and Drives. (3ed). Daniel W. Hart, Prentice Hall International Inc. UK.
- [67] Kjaer, S. B., Pederson, J. K. and Blaabjerg, F. (2005). A review of single-phase gridconnected inverters for photovoltaic modules. IEEE transactions on industry applications, 5(40), 1292-1306.
- [68] Calais, M., Myrzik, J., Spooner, T. and Agelidis, V. (2002). Inverters for single-phase grid connected photovoltaic systems – an overview. Power Electronics Specialists Conference IEEE 33rd Annual, (4), 1995 – 2000.

APPENDICES

Sample of source code used to calculate I_{ph} in model one adapted from [21].

```
function Ia = NT111(Va,G,T)
% G = num of Suns (1 Sun = 1000 W/m^2)
% T = Temp in Deg C
k = 1.38e-23;           % Boltzman's const
q = 1.60e-19;          % charge on an electron
A = 1.2;                % "diode quality" factor, =2 for crystalline, <2
Vg = 1.12;              % band gap voltage, 1.12eV for Si,
Ns = 36;                % number of series connected cells (diodes)
Np=1;                  %number of parallel connected cells (diodes)
T1 = 273 + 25;
Voc_T1 = Vo /Ns;        % open cct voltage per cell at temperature T1
Isc_T1 = Isc;           % short cct current per cell at temp T1
T2 = 273 + 75;
Voc_T2 = Vo /Ns;        % open cct voltage per cell at temperature T2
TaK = 273 + TaC;        % array working temp
TrK = 273 + 25;         % reference temp
Iph_T1 = Isc_T1 * Suns;
a = (Isc_T2 - Isc_T1)/Isc_T1 * 1/(T2 - T1);
Iph = Iph_T1 * (1 + a*(TaK - T1));
Vt_T1 = k * T1 / q; % = A * kT/q
Ir_T1 = Isc_T1 / (exp(Voc_T1/(A*Vt_T1))-1);
Ir_T2 = Isc_T2 / (exp(Voc_T2/(A*Vt_T1))-1);
b = Vg * q/(A*k);
Ir = Ir_T1 * (TaK/T1).^(3/A) * exp(-b.*(1./TaK - 1/T1));
X2v = Ir_T1/(A*Vt_T1) * exp(Voc_T1/(A*Vt_T1));
dVdI_Voc = - 1.15/Ns / 2;
Rs = - dVdI_Voc - 1/X2v; % series resistance per cell
% Ia = 0:0.01:Iph;
Vt_Ta = A * 1.38e-23 * TaK / 1.60e-19; % = A * kT/q
```


Table A1 Sample of the back of panel temperature at June.

Ambient Temperature (°C)	Solar Panel Temperature (°C)	ΔT (°C)
31.00	38.50	7.50
34.60	44.00	9.40
32.20	40.00	7.80
31.00	42.00	11.00
29.40	37.00	7.60
34.00	45.00	11.00
36.30	45.10	8.80
36.50	46.00	9.50
34.70	44.00	9.30
30.90	37.00	6.10
33.30	44.80	11.50
30.50	38.50	8.00
32.87	41.83	8.96